



Monomeric Alkoxo and Alkylcarbonate Complexes of Nickel and Palladium Stabilized with the ⁱPrPCP Pincer Ligand: A Model for the Catalytic Carboxylation of Alcohols to Alkyl Carbonates[†]

Luis M. Martínez-Prieto, Pilar Palma, and Juan Cámpora*

Received 00th January 20xx,
Accepted 00th January 20xx

DOI: 10.1039/x0xx00000x

www.rsc.org/

Monomeric alkoxo complexes of the type [(ⁱPrPCP)M-OR] (M = Ni or Pd; R = Me, Et, CH₂CH₂OH; ⁱPrPCP = 2,6-bis(diisopropylphosphino)phenyl) react rapidly with CO₂ to afford the corresponding alkylcarbonates [(ⁱPrPCP)M-OCOOR]. We have investigated the reactions of these compounds as models for key steps of catalytic synthesis of organic carbonates from alcohols and CO₂. The MOCO-OR linkage is kinetically labile, and readily exchanges the OR group with water or other alcohols (R'OH), to afford equilibrium mixtures containing ROH and [(ⁱPrPCP)M-OCOOH] (bicarbonate) or [(ⁱPrPCP)M-OCOOR'], respectively. However, [(ⁱPrPCP)M-OCOOR] complexes are thermally stable and remain indefinitely stable in solution when these are kept in sealed vessels. The constants for the exchange equilibria have been interpreted, showing that CO₂ insertion into M-O bonds is thermodynamically more favorable for M-OR than for M-OH. Alkylcarbonate complexes [(ⁱPrPCP)M-OCOOR] fail to undergo nucleophilic attack by ROH to yield organic carbonates ROCOOR, either intermolecularly (using neat ROH solvent) or in intramolecular fashion (e. g., [(ⁱPrPCP)M-OCOOCH₂CH₂OH]). In contrast, [(ⁱPrPCP)M-OCOOMe] complexes react with a variety of electrophilic methylating reagents (MeX) to afford dimethylcarbonate and [(ⁱPrPCP)M-X]. The reaction rates increase in the order X = OTs < IMe << OTf and Ni < Pd. These findings suggest that a suitable catalyst design should combine basic and electrophilic alcohol activation sites in order to perform alkyl carbonate syntheses *via* direct alcohol carboxylation.

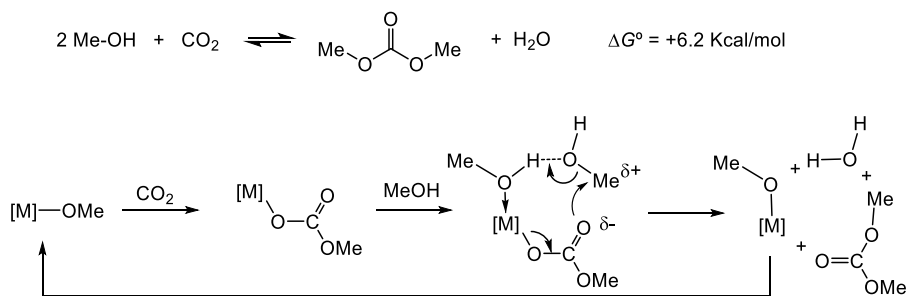
Introduction

There is currently a strong interest in new methods for the production of organic carbonates from carbon dioxide, avoiding the use of phosgene or its derivatives as starting materials.¹ The best developed of such processes involves the reaction of epoxides with carbon dioxide.² This is one of the most promising routes for the incorporation of CO₂ in downstream chemicals and polymers, but epoxides are highly reactive and toxic intermediates, and they are obtained mostly from non-renewable feedstocks.³ Direct carboxylation of alcohols with CO₂ (Scheme 1, up) is an attractive alternative that leads to organic carbonates directly from alcohols, and water as the only by-product.⁴ This is a clean and atom-efficient process that fully complies with the main requisites of green and sustainable chemistry.⁵ Unfortunately, direct combination of aliphatic alcohols with CO₂ to yield alkyl carbonate and water is only weakly exothermic, and endergonic under the ambient conditions (e. g., for methanol $\Delta H^\circ \approx -4$ Kcal·mol⁻¹ and $\Delta G^\circ \approx +6$ Kcal·mol⁻¹ at 1 atm and 298 K) largely due to the unfavorable entropy contribution of gaseous CO₂.^{4,6} The equilibrium constant rapidly decreases

with temperature in such a way that heating to enhance the reaction rate severely limits the maximum theoretical yield, unless the entropy effect is compensated by rising pressure. However, calculations based on standard thermodynamic values have shown that, even at moderately high temperatures, the synthesis of dimethyl carbonate from CO₂ and methanol only becomes exergonic under enormous pressures.^{6b} Therefore, apart from obvious strategies, such as using high CO₂ pressure (ideally, supercritical CO₂ as solvent) or water removal from the reaction mixture (either by physical or chemical methods), the use of efficient catalysts would be essential to allow carbonate formation at the lowest possible temperatures to shift the equilibrium to the right. Various catalysts have been investigated, including both heterogeneous⁷ and homogeneous⁸⁻¹². Among the latter, soluble metal alkoxides,¹⁰⁻¹² in particular diorganotin(IV) dimethoxides (R'₂Sn(OMe)₂)¹¹ and niobium(V) methoxide,¹² are among the most efficient catalysts for the synthesis of dimethyl carbonate from methanol. The mechanisms associated to such catalysts were studied in detail by the groups of Ballivet-Tkatchenko,^{11,13} Aresta^{6a,12b,14} and others.^{4,11} In both cases, the carboxylation process begins with the CO₂ insertion into M-O bonds to afford species containing a methylcarbonate (or hemicarbonato) linkage, [M]-OCOOMe. However, the processes leading to the release of dimethyl carbonate and regeneration of the reactive alkoxo linkage are less well understood. Experimental and computational research on the niobium system suggest that the latter step involves methyl transfer from

[†] Instituto de Investigaciones Químicas. CSIC-Universidad de Sevilla. C/ Américo Vespucio, 49. 41092, Sevilla, Spain.

Electronic Supplementary Information (ESI) available: Further computational details (energies, molecular drawings and atomic coordinates for optimized structures). See DOI: 10.1039/x0xx00000x



Scheme 1.

methanol to the coordinated methoxycarbonyl ligand. As shown in Scheme 1, the acidic metal centre activates two molecules of methanol, which cooperate to propitiate the electrophilic methylation of the negatively polarized methylcarbonate oxygen.^{12a}

Mechanistic studies on the mentioned tin and niobium alkoxide catalysts are complicated because multiple species of different nuclearity coexist in their systems. In addition, the efficiency of such systems is decreased by their low tolerance to water,^{6a,11b,d} with which they react irreversibly to afford insoluble materials devoid of catalytic activity. Well-defined organometallic alkoxide complexes of transition metals provide more accessible systems, better suited for detailed studies of the basic processes involved in catalytic alcohol carboxylation. For example, Bergman¹⁵ and Darensbourg¹⁶ used 18e, coordinatively saturated carbonylrhenium(I) and carbonylmanganese(I) methoxide complexes to ascertain the fundamental mechanistic features of CO₂ insertion into M-O bonds. These studies showed that CO₂ does not bind to the metal prior to insert, but attacks directly on the alkoxide oxygen atom, followed by a fast ligand rearrangement to the alkylcarbonate product.

In recent years, pincer ligands have become a widely used platform for the study of the fundamental reactivity of transition metals.¹⁷ Strong chelating scaffolds such as PCP ligands can efficiently stabilize the otherwise labile hydroxo- or alkoxo species, focusing their reactivity on the M-O bond. Thus, they provide a unique opportunity to explore the details of CO₂ insertion and other elemental processes relevant to alcohol carboxylation.^{18,19} In addition, the stability of the metal-pincer fragment is expected to radically improve tolerance to water, avoiding the coalescence of hydroxo species into insoluble solids.

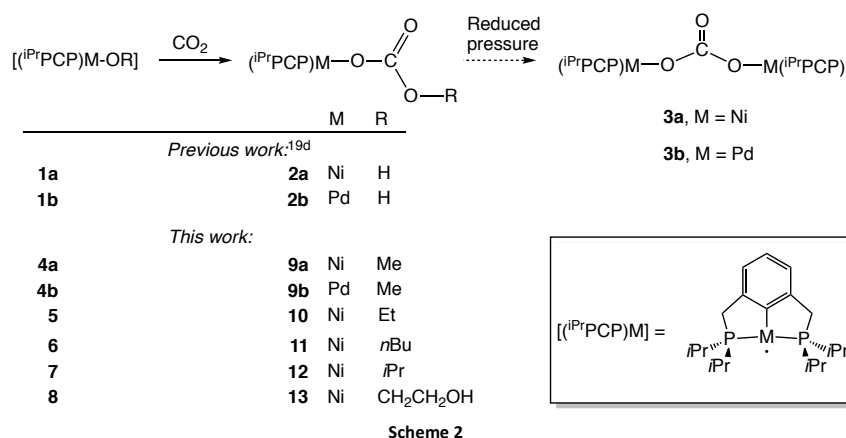
Our group has reported the syntheses of some of the first examples of hydroxide and methoxide complexes of Ni and Pd stabilized with ⁱPrPCP pincer ligands (ⁱPrPCP = 2,6-bis(diisopropylphosphino)phenyl).^{19a,b} We described the reactions of monomeric hydroxo complexes [M(ⁱPrPCP)OH] to afford mononuclear bicarbonate derivatives [M(ⁱPrPCP)OCOOH], and their partial decarboxylation to afford thermally stable binuclear carbonates [{M(ⁱPrPCP)}₂(μ²:κ²-O,O'-CO₃)].^{19d} Next, we studied β-hydrogen elimination reactions in the Ni and Pd methoxides [M(ⁱPrPCP)OMe], which initially lead to the corresponding hydrides [M(ⁱPrPCP)H], and, subsequently, to different M(0) species, depending on M.²⁰ While the Pd methoxide decomposes

readily in alcohol solvents, the nickel counterpart is considerably more stable, particularly when it is dissolved in methanol. Recently, we investigated the hydrolytic stability of a series of nickel and palladium alkoxides showing that Ni complexes are more prone to be hydrolyzed than Pd ones.^{19e} Building on these results, we now report our investigation of such Ni and Pd monomeric alkoxides as models for fundamental reactions of metal alkoxides with CO₂, the thermodynamic relationships between alkylcarbonate and bicarbonate species, and some other processes that could potentially lead to the formation of organic carbonates.

Results and discussion

Reactions of Ni and Pd alkoxide complexes with CO₂ and PhNCO.

As mentioned in the introduction, we have shown that hydroxo pincer complexes [(ⁱPrPCP)M-OH] (M = Ni, **1a** or Pd, **1b**) react with CO₂, quantitatively affording the terminal bicarbonate complexes [(ⁱPrPCP)M-OCOOH] (M = Ni, **2a**; Pd, **2b**).^{19d} Their tendency to undergo partial decarboxylation to the corresponding binuclear carbonates [{(ⁱPrPCP)M}₂(μ²:κ²-O,O'-CO₃)] (**3a** or **3b**, respectively) complicated their isolation. However, taking advantage of their low solubility in hexane, both bicarbonates were crystallized and their X-ray diffraction structures determined. A similar behaviour has been recently reported by Wendt in other Ni-pincer systems.^{18f,g} As shown in Scheme 2, alkoxide derivatives [(ⁱPrPCP)M-OR] (M = Ni or Pd; **4a/b** and **5-8**) exhibit very similar reactivity: when their solutions are exposed to CO₂ they also react rapid and quantitatively affording the corresponding alkylcarbonates **9a**, **9b** and **10-13**. No colour change is observed for the colourless Pd derivative **4b**, but the reddish-orange solutions of the Ni alkoxides rapidly change to yellow. In contrast with the analogous bicarbonates, alkylcarbonate complexes do not precipitate when the reaction is carried out in hexane, in which they are very soluble. However, like the bicarbonates, the alkylcarbonates undergo partial conversion to the corresponding carbonates, **3a** or **3b**, when their solutions are partially concentrated under vacuum. Due to their lower solubility, these binuclear carbonates crystallize preferentially (vide infra). So far, this behaviour has prevented us from isolating pure samples of **9-13**, but NMR characterization was readily accomplished using samples generated *in situ* by bubbling a small amount of dry CO₂ through solutions of the purified alkoxide precursors in C₆D₆. These reactions are very clean; the only other species detected



Scheme 2

were negligible amounts of the corresponding bicarbonate, **2a** or **2b**, arising from water traces. In every case investigated, CO₂ insertion into the M-O bonds was fast and quantitative, as evinced by the clean replacement of the ³¹P{¹H} signal of alkoxides by that of the corresponding alkylcarbonate, usually shifted some 3 ppm downfield from the starting complexes.

The characteristic low-field ¹³C -OC(O)OR carbonyl resonance of alkylcarbonate ligands appears within a narrow region between 157 and 159 ppm. This is shifted by *ca.* 5 ppm upfield from those of the corresponding bicarbonates (~162 ppm). Moreover, CO₂ insertion causes moderate changes to the ¹H and ¹³C signals of the OR moiety. The ¹H spectrum of **13** (Figure 1) provides a remarkable example. This shows two multiplets at δ 4.05 and 3.69, assigned to the CH₂ groups of the glycoxide fragment. The shape of these multiplets indicates that the OCH₂-CH₂O bond does not rotate freely, presumably due to the formation of a rigid structure by intramolecular H-bonding, as previously noted for the parent glycoxide, **8**.^{19e} Yet, in contrast with the broad CH₂ signals of **8**, those of **13** are sharp and well-defined

signals, suggesting that the H bond interaction is stronger in the latter. As shown in Figure 1, the shape of the signals can be simulated by assuming for a rigid AA'XX' spin system characteristic of a stable cyclic system. Notwithstanding, the signals corresponding to the metal-bound (*ipso*) carbon atom of the pincer ligands of alkylcarbonates (M = Ni, 152–153 ppm; Pd, 154.5 ppm) are almost in the same position for alkylcarbonates and bicarbonates, indicating that the influence of the R group on the σ-donor capacity of the -OCOOR (either alkyl or hydrogen) ligand is very small, as expected for partially ionic M-O bonds.^{19e}

In addition to CO₂ insertions, we briefly studied the reaction of the nickel alkoxide **4a** with phenylisocyanate (Scheme 3). ³¹P{¹H} NMR monitoring showed that this reaction also proceeds rapidly to afford a single insertion product, **14**, characterized by a new resonance at δ 52.6. A second, low-intensity ³¹P signal was also observed at δ 56.5. This was attributed to a secondary product arising from the reaction of PhNCO with the small amount of hydroxide **1a** that is usually present in solutions of **4a**. The identity of this species (**14'**) was confirmed by conducting the reaction of **1a** with PhNCO separately. Two features of the ¹H NMR spectrum of **14** suggest that this product is the N-bound (κ¹-N) product arising from C=N insertion, rather than

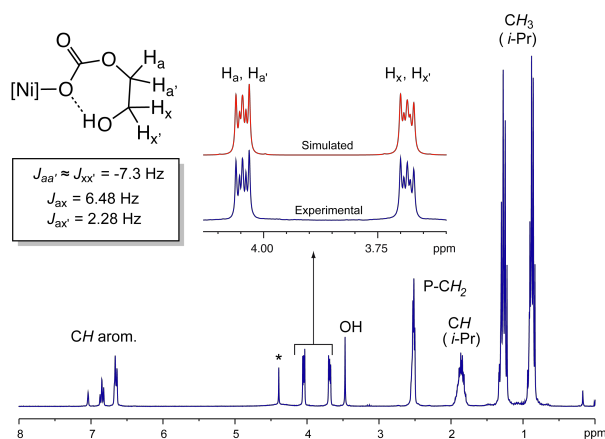
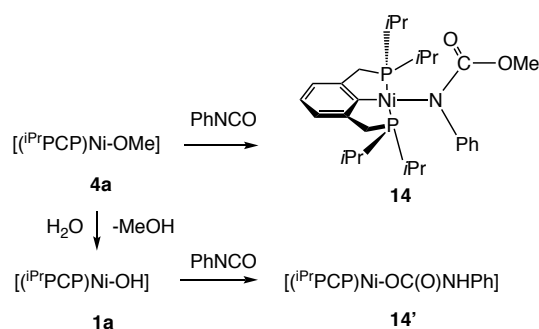


Figure 1. ¹H NMR (300 MHz, C₆D₆, 25 °C) spectrum of compound **13**. The expansion shows the glycoxide CH₂-CH₂ region, and a simulation of the sub-spectrum using the coupling constants indicated in the inset. The * marks a small amount of water.



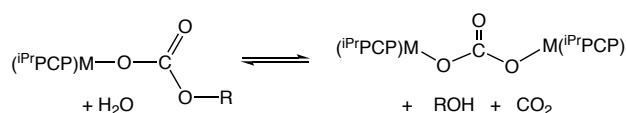
Scheme 3.

its O-bound isomer ($\kappa^1\text{-O}$). First, the *ortho* phenyl protons experience a strong deshielding (δ 8.79) that points to their location near to the axis of the square planar Ni centre. Second, the *N*-phenyl and the pincer isopropyl groups give broad resonances. This is consistent with the restricted rotation of the bulky $\kappa^1\text{-N}$ carbamate ligand with regard to the Ni-pincer fragment, but not with its relatively unhindered $\kappa^1\text{-O}$ isomer. These signals become sharp, well resolved lines when the spectrum is recorded at 55 °C. The same selectivity has been reported for the reactions of isocyanates with different late transition-metal alkoxide complexes.^{15,21} In contrast with the alkylcarbonate complexes arising from CO₂ insertion, both **14** and **14'** are stable and can be isolated as pure microcrystalline solids without decomposition. Hence, PhNCO insertion into the Ni-O bonds of **4a** and **1a** can be regarded irreversible processes, at least under the usual experimental conditions.

Kinetic vs. Thermodynamic Stability of Alkylcarbonate Complexes

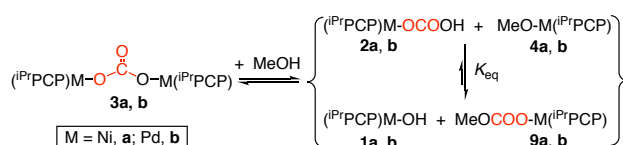
As discussed before, Ni and Pd alkylcarbonate complexes [(ⁱPrPCP)M-OCOOR] are prone to evolve into the corresponding binuclear carbonate **3a** or **3b**, but ascertaining the final fate of the alkoxo (OR) groups was not trivial, because the transformation is usually partial, and they end up in volatile organic products that are not easily detected. By analogy with the decarboxylation of inorganic bicarbonate salts to the corresponding carbonates, one could speculate that the byproducts of the decomposition of alkylcarbonates might be organic carbonates (RO)₂CO or ethers R₂O, the counterparts of carbonic acid and water, respectively. In order to clarify this point, we heated C₆D₆ solutions of the nickel alkylcarbonates **9a** (R = Me), **12** (R = *i*Pr), and **13** (R = CH₂CH₂OH) at 100 °C in NMR sample tubes sealed with gas-tight PTFE valves, recording their ³¹P{¹H} or ¹H NMR spectra at regular intervals for up to 12 h. No changes were observed in the first two samples, indicating that these compounds are thermally very stable provided that loss of volatile components is avoided. In contrast, glycoxide **13** is proved somewhat less stable, as its spectrum decayed and fully disappeared after heating for four days. This appeared potentially interesting, because the glycoxide moiety might be favoring elimination of cyclic ethylene carbonate *via* intramolecular nucleophilic cyclization of the 2-hydroxyethylcarbonate fragment. However, neither ethylene carbonate nor any other organic products were formed in amounts large enough to allow their identification in the final ¹H spectrum of the sample. The only identifiable signals in the final ³¹P{¹H} spectrum were those of the tetranuclear carbonyl [Ni₄(CO)₅(ⁱPrPCHP)₂] and free ⁱPrPCHP ligand, which had been recognized in our previous studies as the signature of the irreversible decomposition of methoxide **4a**. This process involves a complex sequence of steps that ultimately cause full dehydrogenation of the OMe ligand down to CO and the collapse of the [(ⁱPrPCP)Ni] unit.^{20b} From this we deduce that the thermal instability of **13** relates to the properties of the alkoxide (resulting from CO₂ de-insertion), rather than to the sought organic carbonate elimination.

The above-discussed experiments lead us to conclude that alkylcarbonate complexes are thermally stable in solution, at least at the ambient temperature. Their facile transformation into the corresponding binuclear carbonates does only take place when their solutions are allowed to exchange volatile components (*e. g.*, under reduced pressure). In order to monitor these transformations under controlled conditions, we heated an NMR samples of the alkylcarbonate complexes in toluene-*d*₈ at 100 °C, kept in a closed thermostatic vessel purged with a slow N₂ stream, designed to remove CO₂ or other gases while minimizing exposure to air or moisture (see Experimental Section). The samples were periodically removed to measure their NMR spectra. Under these conditions, nickel methylcarbonate **9a** was quantitatively transformed into **3a** within 15 h, but the organic products were also lost. The heavier *n*-butylcarbonate derivative **11** would give more chance to detect less volatile organic products. When **11** was subjected to the same procedure, the transformation took 48 h to complete. The only organic product detected in the ¹H spectra was a small amount of *n*-butanol, that disappeared once **11** was fully consumed. In a separate test, we checked that, despite its high boiling point (118 °C), *n*-butanol gradually leaves a toluene-*d*₈ solution under the conditions of the experiment. Other potential products, like di-*n*-butylcarbonate or di-*n*-butylether, were not detected. Since these even less volatile than *n*-butanol (b. p. 207 and 141 °C, respectively) it can be concluded that the R group is lost exclusively as ROH. To test this proposal, we conducted one further experiment, in which a solution of 0.025 mmol of **9a** in *ca.* 0.7 mL of C₆D₆ was evaporated to dryness, collecting the volatiles in a small trap cooled with liquid nitrogen. NMR analyses showed that the solid residue was a 5:1 mixture of **9a** and **3a**, while the C₆D₆ collected in the trap only contained methanol. As shown in Scheme 4, transformation of alkylcarbonate complexes into the corresponding carbonates and free alcohol requires water. Most likely, this is taken from moisture traces present in the solvents or glassware. However, the advance of the reaction requires removal of the alcohol from the system.



Scheme 4.

Hydrolysis of alkylcarbonate complexes to afford carbonate compounds has been seldom mentioned in the literature,^{22,23} although it might be a common fairly common reaction for late transition metal derivatives. In 1992, Bergman and Simpson showed that rhenium alkylcarbonate complexes react with two equivalents of water at 45 °C to afford a binuclear carbonate derivative.¹⁵ However, such experimental conditions suggest that the latter process was not as facile as the hydrolysis of the Ni and Pd alkylcarbonate derivatives **9** - **13**. Furthermore, in this group 10 system, the hydrolysis is reversible and alkylcarbonates are fully restored upon addition of CO₂ and alcohol to the corresponding binuclear carbonate. In fact, addition of extra



Scheme 5.

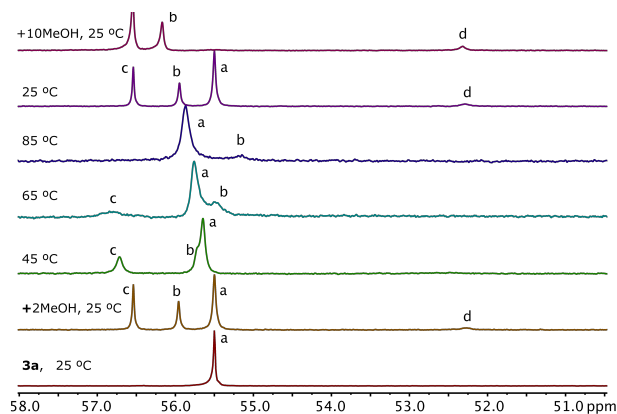


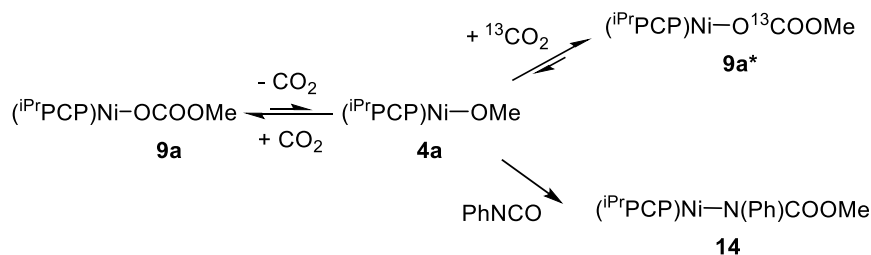
Figure 2. Effect of the addition of methanol on the $^{31}\text{P}\{^1\text{H}\}$ spectrum of **3a** at different temperatures. Starting from the bottom: i) spectrum **3a**; ii) addition of MeOH (2 eq.); iii – vi) the same spectrum recorded at 45, 65 and 85 °C, and again at room temperature; vii (top), excess MeOH (10 Equiv). Key to signals: a: carbonate (**3a**); b: hydroxide (**1a**); c: methylcarbonate (**9a**) + bicarbonate (**2a**); d: methoxide (**4a**).

CO_2 is not strictly required. Thus, Ni or Pd carbonates **3** in C_6D_6 solution react instantly with stoichiometric amounts of MeOH to afford equilibrium mixtures containing **9** and hydroxide **1**, together with minor amounts of the corresponding bicarbonate (**2**) and methoxide (**4**), as shown in Scheme 5. The different species in the equilibria were identified by comparison of their ^1H and $^{31}\text{P}\{^1\text{H}\}$ NMR signals with those of authentic samples, and the equilibrium condition was confirmed by studying the perturbation of the system by changes in the temperature and the **3** / MeOH ratio. Figure 2 illustrates these experiments for the nickel derivative **3a**. As long as the amount of methanol added is close to stoichiometry (*i. e.* $[\text{M}]:\text{MeOH} \approx 1:1$), the equilibrium mixture contains measurable amounts of each of the equilibrium components. At the room temperature, the signals exhibit some broadening due to the intermolecular exchange. As expected, these effects become more evident as the temperature is increased, but the original spectrum is reproduced when the sample is cooled again to 25 °C. Addition of a large excess of methanol (10-fold) shifts the equilibrium to the right side, removing the resonance of the carbonate complex.

From a mechanistic point of view, the reaction of the Ni or Pd carbonates with methanol can be seen as a protolytic cleavage

of one of the M-O bonds of the strongly basic carbonate complex. Initially, this should generate a 1:1 mixture of the corresponding methoxide **4** and bicarbonate **2**, that subsequently equilibrates with the hydroxide / methylcarbonate pair **1** / **9**. The whole process is so fast that all products appear to be formed simultaneously. Actually, the equilibrium constant K_{eq} favors the **1** / **9** pair (*i. e.*, $K_{\text{eq}} \gg 1$). This circumstance may give the false impression that methanol breaks one of the carbonate-metal fragments, to afford methylcarbonate **9** and hydroxide **1** (see spectrum *ii* in Figure 2). This could suggest that, under more strict conditions, the same process could be forced to proceed in the remaining M-O bond to afford dimethyl carbonate and hydroxide, **1**. Nevertheless, despite our many efforts, such a reaction was never observed (see below).

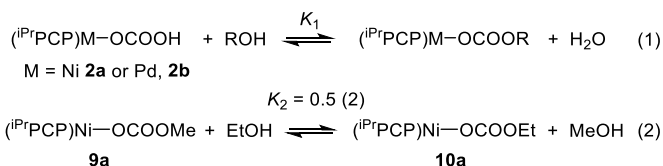
Rapid equilibration of the species placed within the braces at the right side of Scheme 5 implies that CO_2 “jumps” freely from one molecule to another, exchanging the insertion site between M-OH and M-OMe. Most likely, the mechanism of CO_2 transfer implies reversible elimination and re-insertion of this molecule. In a previous article, we showed that, in fact, CO_2 insertion can be reverted for bicarbonates, **2**, to afford the corresponding hydroxides, **1**.^{19d} However, despite the lability of alkylcarbonates (**9-13**), we have never observed *directly* the reversal of CO_2 insertion into metal-alkoxide bond. That is to say, we could not detect alkoxides $[(^i\text{PrPCP})\text{M-OR}]$ being formed by CO_2 extrusion from the alkylcarbonate $[(^i\text{PrPCP})\text{M-OCOOR}]$ complexes. In the literature, the reversibility of CO_2 insertion into metal-alkoxide bonds has been supported with isotope labelling experiments, using ^{13}C -labelled CO_2 .^{15,16} In the same vein, we performed an experiment bubbling dry $^{13}\text{CO}_2$ through a solution of **9a** in C_6D_6 . A rapid enhancement of the Ni-OCOOME carbonate resonance took place in the ^{13}C NMR spectrum. This demonstrates the intermolecular CO_2 exchange, that apparently takes place as shown in Scheme 6. However, a control experiment revealed that this test could be deceptive. According to the proposed mechanism, binuclear carbonate **3a** should not be able to exchange CO_2 , because this compound is reluctant to eliminate CO_2 even under forcing conditions^{19d} (such a process would lead to a high-energy, unprecedented μ -oxo Ni(II) species). Yet, **3a** exchanges $^{13}\text{CO}_2$, at a comparable rate to that observed in the case of **9a**. We believe that this exchange is actually catalysed by small amounts of nickel bicarbonate complex **2a**, in equilibrium with **3a**. The impurity of **2a** appears unavoidable, despite of our efforts to thoroughly dry the $^{13}\text{CO}_2$ by storage over P_2O_5 or concentrated H_2SO_4 for a long period of time (up to 2 months). The same mechanism could be responsible for the



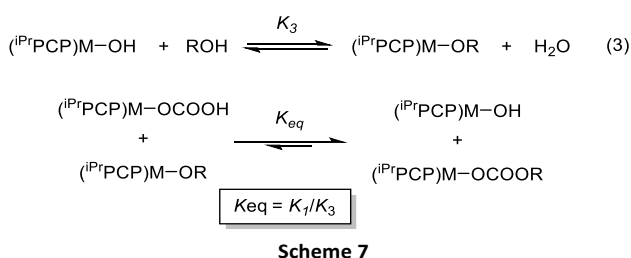
Scheme 6.

$^{13}\text{CO}_2$ exchange in the case of **9a**. We finally gained evidence for the reversibility of the CO_2 insertion into the Ni-OMe bond by performing a different kind of exchange experiment, in which **9a** was reacted with PhNCO to afford carbamate complex **14**. In this case, the irreversibility of isocyanate insertion, either into Ni-OMe or Ni-OH bonds, rules out any potential route catalysed by the bicarbonate impurity (Scheme 6). Monitoring the reaction of **9a** with PhNCO in a gas-tight NMR tube showed that, although initially fast, it becomes noticeably slower as the reaction advances, nearly stopping at 40 % conversion. This is expected if a CO_2 elimination/insertion equilibrium precedes the irreversible PhNCO insertion, as the released CO_2 accumulates in the sample tube. Similar conclusions have been reached by other authors when comparing the insertion reactions of CO_2 into M-OR bonds with those of CS_2 or other heterocumules.^{15,21c}

As a consequence of the kinetic lability of CO_2 insertion, bicarbonates and alkylcarbonates are readily exchangeable. We checked that both bicarbonates **2a** and **2b** do in fact react with methanol, affording equilibrium mixtures containing the methylcarbonate and water. This kind of process is in fact very general, as both bicarbonates **2** do react similarly with different alcohols, as shown in Eq. 1. Not only bicarbonates but also alkylcarbonates exchange readily with different alcohols, as illustrated by the exchange of **9a** with ethanol (Eq. 2). These reactions can be compared with classic esterifications and transesterifications, but their different nature is revealed by their very different rates. Carboxylic acids and esters usually undergo these reactions much more slowly, even in the presence of catalysts, while the “inorganic” versions shown in Eqs 1 and 2 are essentially instantaneous at the room temperature. Equilibrium concentrations are attained shortly after mixing the reagents.



In a previous work, we determined the equilibrium constants for the process described in Eq. 3 (K_3) using $^{31}\text{P}\{^1\text{H}\}$ NMR-based titration of the hydroxide complexes (**1a** or **1b**) with the corresponding alcohol.^{19e} The same method proved useful to determine the equilibrium constants for Eq 1 (K_1), taking advantage of the ready availability of both Ni and Pd bicarbonates **2** as pure, crystalline materials. Combining Eq 1 with the reversal of



Eq 3, one obtains the equilibrium shown in Scheme 7, whose equilibrium constant K_{eq} equals the ratio K_1/K_3 . This process is interesting because it provides a measure of the relative tendency of CO_2 to insert into M-OR or M-OH bonds. Note that this is the same partial equilibrium shown within brackets in Scheme 5, which, in a real experiment, cannot be isolated from the complication posed by the formation of carbonate species (**3**).

A potential problem for the bicarbonate titration experiments is that the ^{31}P resonances of the bicarbonate and alkylcarbonate derivatives do appear very close, and in some situations, like the carbonate-methanol exchange (see Figure 2), these may coalesce in a single peak (signal labeled “c”). However, in contrast with these spectra, the processes described in Eqs 1 and 2 involve only two ^{31}P sites. As a consequence, in these experiments the $^{31}\text{P}\{^1\text{H}\}$ signals appear narrow enough to be integrated individually. Thus, we undertook K_1 measurements for the exchanges of **2a** and **2b** with methanol, ethanol and 2-methoxyethanol (the latter was selected as a simplified surrogate of the glycoxide, in order to avoid strong intramolecular hydrogen bonds). Only the equilibrium corresponding to the reaction of **2a** with ethanol (K_1 Ni, EtOH) posed serious problems for the integration of the $^{31}\text{P}\{^1\text{H}\}$ signals, but in this case the value of the equilibrium constant was estimated indirectly, as K_1 (Ni, EtOH) = $K_2 \times K_1$ (Ni, MeOH).

Table 1 collects the values of K_1 and K_{eq} , determined as discussed above, and Table 2 compares Gibbs free energies, ΔG° , corresponding to the K_{eq} with theoretical values computed applying DFT methods validated in our previous work for Eq. 2.^{19e} There is reasonable agreement between the experimental and theoretical set of data, and the trends are well reproduced by the DFT calculation, reinforcing our confidence in the general validity of the set of K_{eq} data. In addition, Table 2 displays temperature-independent energy balances $\Delta E(\text{SCF}+\text{ZPE})$, that can be related to the enthalpy term. These are not very different from the experimental ΔG° values, indicating that the contribution of thermal corrections is small. Doubtless, this circumstance contributes to the good agreement between experimental and computational data, as the thermal corrections for DFT in solution phase are only approximate.

As can be seen in Table 1, K_1 values are about two orders of magnitude larger than those of K_3 (the alcohol exchange), implying that bicarbonate-alkylcarbonate equilibria (1) are much closer to thermoneutral than hydroxide-alkoxide (3). This observation can be readily justified in the light of our previous work.^{18e} In brief, the trends in the K_3 and K_1 depend on the different intensity in which the R group influences the thermodynamic stability of the partially ionic

Table 1. Bicarbonate/Alcohol Equilibrium constants, K_1 and K_{eq} .

	MeOCH ₂ CH ₂ OH	MeOH	EtOH
K_1 , Ni	0.23(4)	2.6(5)	1.3(3) ^a
K_1 , Pd	0.20(3)	1.7(4)	0.5(1)
K_3 , ^b Ni	$5.7(2) \times 10^{-3}$	$1.6(3) \times 10^{-2}$	$1.4(2) \times 10^{-3}$
K_3 , ^b Pd	$5.0(10) \times 10^{-2}$	$4.5(6) \times 10^{-2}$	$2.6(8) \times 10^{-2}$
K_{eq} , ^c Ni	40(7)	160(40)	930(30)
K_{eq} , ^c Pd	4(1)	38(9)	19(7)

a) Calculated as K_1 (Ni, MeOH) \times K_2 . b) taken from ref. ^{19e}. c) $K_{\text{eq}} = K_2/K_3$

Table 2. Experimental^a and DFT^b energy balances for Eq. 3 (Kcal·mol⁻¹)

	Me- OCH ₂ CH ₂ OH	MeOH	EtOH
ΔG° exp., Ni	-2(1)	-3.0(9)	-4.0(9)
ΔG° DFT, Ni	-1.4	-4.5	-4.8
ΔE (SCF + ZPE), Ni	-2.2	-3.6	-3.9
ΔG° exp., Pd	-0.82(9)	-2.1(9)	-1.7(8)
ΔG° DFT, Pd	+0.7	-2.4	-1.5
ΔE (SCF + ZPE), Pd	+0.1	-1.5	-0.5

a) ΔG° exp. = $-RT \cdot \ln(K_{eq})$. b) PBE (6-31+G*, CPCM)//6-311++G(3df, 2p), CPCM)

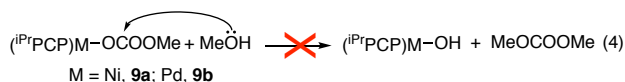
M^{δ+}-O^{δ-} bonds. When comparing alkoxides and hydroxides, the ability of a polarizable R groups disperse the excess of negative charge that resides on the oxygen atom of alkoxides, decreases the coulombic attractive force that makes up for a significant part of the M-OR bond strength. The consequence is that the small and negatively charged hydroxide anion binds more strongly to the cationic metal fragment than an alkoxo OR ligand. This results in a significant destabilization of the alkoxides relative to hydroxides, hence in small values of K_3 . In contrast, the R has a comparatively minor influence on the electrostatics of the M-OCOR linkage, therefore the strength of the M-O bonds in alkylcarbonates and bicarbonates is alike, and K_1 values are closer to unit. Since the values of K_3 are much smaller than K_1 , the equilibrium constant K_{eq} ($= K_1/K_3$) are quite large. Moreover, since K_{eq} are dominated by K_3 , these show similar trends but in opposite directions. Because the Ni(II) atom has a smaller size than Pd(II), electrostatic effects are more marked for the former, resulting in comparatively larger K_{eq} values in the nickel system.

Even though the experimental values of K_{eq} have relatively large uncertainties, our results plainly indicate that the thermodynamics of CO₂ insertion favors the formation of alkylcarbonate (M-OCOR) over bicarbonates (M-OCOOH). This is an intuitive concept, as it merely confirms that CO₂ insertion takes place more readily into the weaker alkoxide M-OR bond than in the stronger M-OH bond of hydroxides. Furthermore, since hydroxides, alkoxides and their CO₂ insertion products are labile and rapidly exchanging in solution, it can be concluded that under typical catalytic conditions, *i. e.*, alcohol as the solvent and high CO₂ pressure, the alkylcarbonate M-OCOR will always be the prevailing species. Since the value of K_{eq} is dominated by the inverse of K_3 , the preference for the alkylcarbonate complex increases in the order Pd < Ni and MeOCH₂CH₂OH < MeOH < EtOH. Furthermore, it is expected that the tendency to form the alkylcarbonate species will be stronger for less acidic alcohols, like *i*PrOH.

Formation of Organic Carbonates

We have investigated two types of processes that may potentially cause the displacement of alkylcarbonate ligands as organic alkylcarbonates: nucleophilic attack by the alcohol, and electrophilic alkylation (Scheme 8). We show in this section that, even though pincer alkylcarbonates are unreactive in the first of these two

Nucleophilic displacement:



Electrophilic displacement:



M = Ni, **9a**; Pd, **9b**

X = I, M = Ni, **15a**; Pd, **15b**
X = OTf, M = Ni, **16a**; Pd, **16b**
X = OTs, M = Ni, **17a**; Pd, **17b**

Scheme 8

pathways, they do react with electrophiles to afford organic alkyl carbonates.

As expected, when hydroxides **1a** and **1b** are dissolved in methanol-*d*₄ and exposed to 4 bar of dry CO₂ in thick-walled pressure NMR tubes, they are fully converted into the corresponding methylcarbonate complexes, **9a** or **9b**. In order to generate dimethylcarbonate, these products should be able to react further with methanol, according to Eq 4 (Scheme 8). This reaction would regenerate the starting hydroxides, initiating a catalytic cycle. Therefore, in an attempt to force such processes, the NMR samples were heated to 80 °C, and their ³¹P{¹H} and ¹H NMR were recorded at regular intervals. The colour and the spectra of the samples of the nickel complex remained essentially unchanged over prolonged heating (24 h), indicating that **9a** is stable under the experimental conditions, but those prepared from the Pd derivative become gradually dark, at the same time that ³¹P{¹H} signals for **9b** complex faded away. The different stabilities of the Ni and Pd methylcarbonates parallels the previously investigated behaviour of the corresponding methoxides **4** in methanol,^{20b} suggesting that **4b** may be involved in the decomposition of **9b**. GC-analyses of the samples did not reveal the presence of dimethyl carbonate in neither of these experiments (M = Ni or Pd). The possibility that dimethyl carbonate could be formed, but immediately degraded back to methanol and CO₂ was definitively ruled out by means of an isotope labeling experiment: a solution containing dimethylcarbonate and hydroxide **1a** in methanol-*d*₄ was heated at 80 °C under 4 bar of dry ¹³CO₂. If any dimethyl carbonate had been formed under these conditions, the label would have been incorporated, and a significant enhancement of the MeOCOOMe resonance would have been observed in the ¹³C NMR spectrum of the mixture. However, the intensity of this signal remained unaltered after heating for > 2 days. In contrast, we did observe some decay of the intensity of the ¹H CH₃ signal of dimethyl carbonate was observed to decay over time, which we attribute to the exchange of the methoxy groups of the deuteromethanol used as solvent.

The negative results of the precedent experiments were not surprising, because the endergonic character of the reaction of CO₂ with methanol severely limits the feasibility of the catalytic cycle under the mild pressures accessible in an NMR tube. To improve the chances of detecting the formation of dimethyl carbonate, we carried out reactions at 20 atm of CO₂ at 80 and 100 °C in steel reactors, using neat methanol as a solvent. The final mixtures were analyzed using ³¹P{¹H} and GC-MS. In addition,

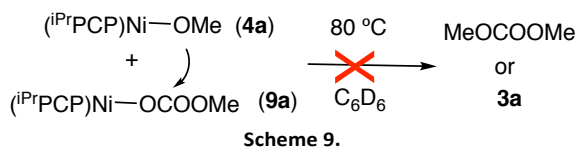
Table 3. Yields and rates for the reactions of **9a** and **9b** with MeX (60 °C, C₆D₆).
$$(\text{iPrPCP})\text{M}-\text{OCOOMe} + \text{MeX} \xrightarrow[\text{(traces of H}_2\text{O)}]{k} (\text{iPrPCP})\text{M}-\text{X} + \text{MeOCOOME} (+ \text{MeOH} + \text{CO}_2)$$

M	X	MeX/ [M]OCOOME	Me ₂ CO ₃ (%) ^a	MeOH (%) ^a	Me ₂ CO ₃ + 0.5·MeOH,%	T ₅₀ ^b	Rate (k) x 10 ⁶ ^c
Ni	I	1:1	36	52	62	>1000	-- ^d
Ni	I	10:1	50	40	70	240	8 ^e
Ni	I	15:1	74	19	83	50	40 ^e
Ni	I	20:1	45	54	72	29	68 ^e
Ni	OTs	10:1	68	10	73	2100	5
Ni	OTs	20:1	83	7	86	410	29
Ni	OTf	1:1	86	22	97	-- ^f	-- ^f
Pd	I	10:1	68	30	83	90	121
Pd	I	20:1	88	20	98	11	1070
Pd	OTs	10:1	65	9	69	1500	8
Pd	OTs	20:1	56	3	57	110	109
Pd	OTf	1:1	81	28	95	-- ^f	-- ^f

a) ¹H NMR yields, % with regard to the converted organometallic complex. b) time for 50 % consumption of the starting material, min. c) first order apparent rate constants unless otherwise stated. d) slow reaction. e) apparent 1/2-order rate constants, (mol/L)^{1/2}·s⁻¹. f) fast reaction.

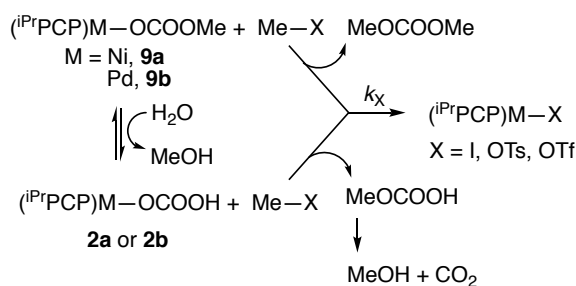
we attempted the carboxylation of methanol or ethyleneglycol using sc-CO₂ at 170 °C. In either case, the Pd catalyst (generated from **1b**) decomposed under the reaction conditions, while the nickel catalyst generated from **1a** led to yellow solutions containing mostly the corresponding alkylcarbonate species, **9a** or **13**, but no organic carbonates were formed.

The lack of activity of the nickel complexes in the presence of methanol and CO₂, under various conditions, indicates that the alkylcarbonate ligand (*i.e.*, M-OCOOR) is unable to experience nucleophilic attack by the alcohol, even if this might happen intramolecularly (when R = CH₂CH₂OH). In an attempt to further explore the reactivity of alkylcarbonates towards nucleophilic attack, we confronted **9a** with the methoxide complex **4a**, a much stronger nucleophile than methanol itself. With this aim, we reacted a solution of **4a** in C₆D₆ with a volume of CO₂ corresponding to *ca.* 0.5 equiv., to generate a sample containing approximately equimolar amounts of **4a** and **9a**. The sample was sealed in a gas-tight PTFE valve NMR tube and heated at 80 °C. No carbonate products were produced (neither dimethyl carbonate, nor the carbonate complex **3a**, see Scheme 9). Under the conditions applied, the only process observed was the thermal decomposition of the methoxide **4a**, that takes place as reported before.^{20b}



As mentioned above, Lewis-acidic catalysts can activate methanol to behave as an electrophilic methylating agent (Scheme 1). Such a mechanism is unlikely in the case of the mildly Lewis acidic, 16-electron Ni(II) or Pd(II) alkylcarbonate complexes. Notwithstanding, once we established the inability of nickel al-

kylcarbonate complexes to undergo nucleophilic attack with alcohols, we decided to explore the opposite approach and investigated the reactions of **9a** and **9b** with a variety of electrophilic alkylating reagents: methyl iodide, methyl tosylate and methyl triflate (see Eq. 5 in Scheme 8). The experiments were carried out at 60 °C in gas-tight NMR tubes. Solutions of Ni and Pd methylcarbonate complexes **9** were generated *in situ* bubbling a small excess of CO₂ through 0.3 M solutions of the corresponding alkoxides, **4a** or **4b** in C₆D₆. The progress of such reactions was monitored using both ³¹P{¹H} and ¹H NMR. Table 3 collects rate and selectivity data for these reactions. As observed through the ³¹P channel, the reactions appear straightforward, the signal of the starting material being cleanly replaced by that of the corresponding complexes [(ⁱPrPCP)M-X] (M = Ni, Pd; X = I (**15a/b**), OTf (**16a/b**) or OTs (**17a/b**)), identified by comparison with authentic samples of such compounds prepared independently (see Experimental Section). The simplicity of these ³¹P{¹H} spectra provide a convenient method to monitor the progress of the reactions. In contrast, the ¹H channel showed that the expected organic product, dimethyl carbonate (singlet at δ 3.72 ppm), is usually formed along with some methanol (overlapping signals at δ 3.04 and 3.05 for Me and OH, respectively). No other organic products were detected. The ratio of dimethyl carbonate to methanol varies strongly, depending on the metal complex and the reagent used, and in general it does



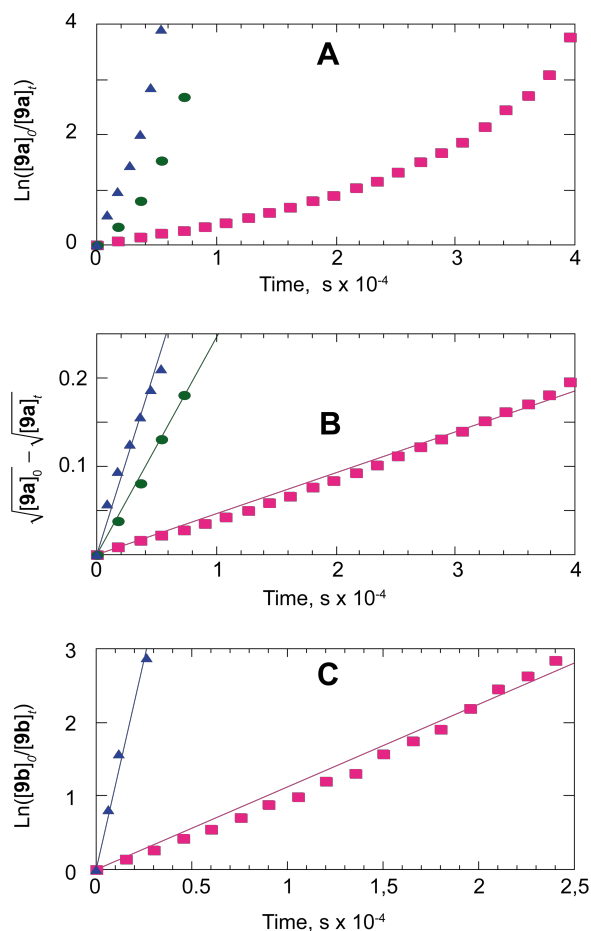


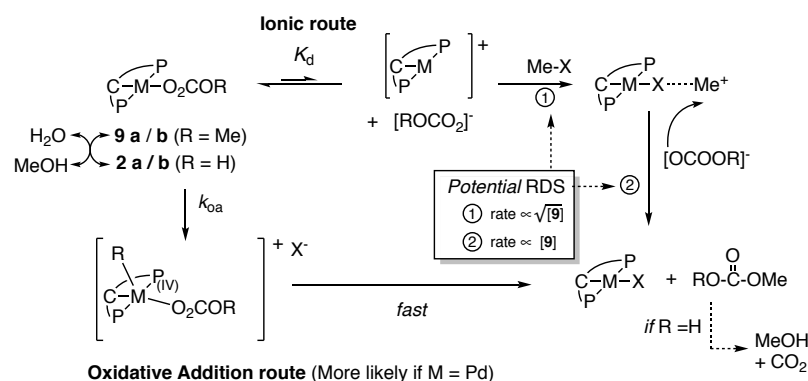
Figure 3. Kinetic plots for the reactions of methylcarbonate complexes **9a** and **9b** with MeI at 60 °C (C_6D_6). The plots mark the disappearance of the ^{31}P signal of the starting complex. $[M]:[IME]$ ratio = 1:10 (\blacksquare), 1:15 (\bullet), 1:20 (\blacktriangle). **A:** First order plots for $M = Ni$ (**9a**); **B:** Same data as **A**, in a 0.5-order plot; **C:** First order plot for $M = Pd$ (**9b**).

not correlate to the amount of alkylating reagent used. The latter observation rules out the possibility that methanol could arise from traces of acid (HX) in the alkylating reagents (MeX). A more likely explanation is that MeOH arises from the competitive methylation of the ubiquitous bicarbonates **2**, as methylcarbonic acid is unstable and readily dissociates into the free alcohol and CO_2 .²⁴ To explain the relatively large amounts of methanol formed in some of these reactions, we assume that bicarbonates react with the methylating reagent more rapidly than methylcarbonates. This proposal is supported by the early disappearance of the small ^{31}P signal of the bicarbonate impurity, within the initial minutes of each experiment. The competition between alkylation and hydrolysis equilibrium leads to more efficient water capture when the former reaction is slow, as shown in Scheme 10. Note that a single molecule of **4a/b** leads to the net production of two equivalents of methanol. The palladium methylcarbonate **4b** is appreciably more reactive towards electrophiles than that of nickel, **4a**, but reaction rates

show the same trend for both complexes, increasing in the order MeOTf < MeI << MeOTf. Under the conditions applied, reactions with MeOTf are too fast to allow direct NMR monitoring. In the other two cases, we anticipated that the decay of the ^{31}P resonance of the starting material would exhibit first-order kinetic dependencies both on the metal complexes and the electrophile. Accordingly, these would exhibit simple pseudo-first order kinetics if the electrophile / complex ratio is large enough (10:1 or higher), and the apparent rate constant would increase proportionally to the initial electrophile concentration. However, rather more complex kinetic behaviour was observed.

Although most experiments gave reasonably linear first-order kinetic plots, those for the reactions of the nickel complex **9a** with MeI showed evident deviations (see Figure 3). Such kinetic behaviours are best described with a kinetic order of 0.5 on **9a**. In contrast, the first order plot for the palladium complex, **9b** shows only minor deviations. Apparent rate constants (pseudo-first or -half order) are listed in Table 3, together with T_{50} (time required to convert 50 % of the starting complexes **9**). As expected, reaction rates increase with the initial concentration of the electrophile but, surprisingly, the increases are in all cases much more pronounced than the expected for a simple first order dependency. We believe that this is probably a bulk solvent effect rather than a genuine kinetic dependency, as for 10-20 fold excess of MeX, this reagent represents a significant fraction (5 -10 %) of the total volume, which has important effects on the polarity and solvating properties of the medium in relation to neat C_6D_6 .²⁵

Among the conceivable mechanisms for the reactions of organometallic compounds with electrophiles, three of them appear more likely for the reaction of **9a/b** with MeX: (i) direct electrophilic attack on the coordinated methylcarbonate ligand; (ii) oxidative alkylation of the electrophile to the M(II) centre, followed by $Me\cdots OC(O)Me$ reductive coupling at the resulting M(IV) intermediate, and (iii) free radical mechanisms including an initial outer sphere electron transfer step.²⁶ The latter possibility is more likely for Ni complexes. However, the comparatively much higher reactivity MeOTf than IMe seems to point to a mechanism of type (i) and (ii) for both Ni and Pd.²⁷ Seeking some additional proof in favor or against mechanism (iii), we carried out reactions of **9a** and **9b** with 1-iodohexen-5-ene, a typical "radical clock" test for free radicals.^{26,28} Such reactions yield the expected iodocomplexes **15**, but the organic outcome was less clean than with methylating electrophiles. For palladium (**9b**), the main organic product identified in the 1H spectrum was the cross-coupled carbonate $Me-OCO(CH_2)_4CH=CH_2$,²⁹ identified on the basis of its characteristic signals, a low field triplet (δ 4.06) and singlet (δ 3.48) for to the $OC(O)O-CH_2-C_5H_9$ and CH_3-OCO groups, respectively. For Ni (**9a**), the 1H spectrum showed an ill-defined mixture of organic products and the amount of the mixed carbonate was small. However, in none of these reactions we detected diagnostic doublet signals between 2.5 and 3.5 ppm, expected for the *exo*-methylene group of any cyclopentyl products of the type $X-CH_2-cyclo-C_5H_9$ ($X = MeOC(O)O-$



, HO-, I- etc), that would be produced if the mechanism involved free methyl-5-hexen-1-yl radical as an intermediate.²⁸ This result can be taken as a negative "radical clock" test, and confirmed our previous impressions, in the sense that radical mechanisms are not playing any relevant role in these electrophilic ligand alkylations.

The first order kinetic dependency on RX observed in most of these reactions is uninformative, as it is equally compatible with direct alkylation of the -OCOOMe ligand (mechanism *i*), or oxidative addition followed by reductive elimination (mechanism *ii*). However, the fractional $\frac{1}{2}$ -kinetic order observed in the reactions of **9a** with MeI is peculiar, and points to some less usual pathway. This feature is strongly reminiscent for mechanisms in the upper part of Scheme 11. Ionization of the methylcarbonate/bicarbonate ligand generates a coordinatively unsaturated cationic metal species, $[(iPrPCP)M]^+$. Coordination of the electrophile (step marked "1") activates the X-Me bond towards nucleophilic attack by the counteranion, $[ROCO_2]^-$ to yield $[(iPrPCP)MX]$ and the organic carbonate (step "2"). In favour of such a mechanism, it could be argued that some soft metal cations (e. g. Ag^+ or Hg^{2+}) are known to promote substitution reactions on alkyl halides R-X.^{19c,27,30} Note that the relative rates of steps 1 and 2 control the kinetic order of the overall process. When step 1 is rate-determining (RDS) the overall reaction rate depends on the concentration of the cationic intermediate, hence the $\frac{1}{2}$ -order kinetic dependency on **9**. This could be the situation when the electrophile is IMe, a very poor ligand. On the other hand, with a more coordinating electrophile like methyl tosylate, step 2 would become RDS. In this case, overall first-order dependency on the starting complex (**9**) would be observed. In general, the RDS role of steps 1 or 2 might not be clear-cut, resulting in the observed deviations from ideal rate laws. It is worth recalling that a simple first-order dependency would be also compatible with other mechanisms, such as the oxidative addition step, also drawn in Scheme 11 (bottom). This would be more feasible for Pd^{26,31} than for Ni.³² The RDS in this mechanism should be the oxidative addition step (k_{OA}), also leading to an ionic pair. Therefore, the influence of the medium polarity on both oxidative addition and the dissociative routes. Finally, methanol production is readily accommodated in this

mechanistic scenario assuming that **9** equilibrates with **2**, as described above.

Conclusions

In this study, we have investigated the interaction of CO₂ with monomeric nickel and palladium alkoxide complexes stabilized with the *iPr*PCP pincer ligand, and their potential as a model to improve our understanding of the fundamental steps of catalytic alcohol carboxylation.

We have shown that insertion of CO₂ into the M-O bonds of Ni and Pd alkoxides is essentially instantaneous and quantitative. The resulting alkylcarbonate complexes $[(iPrPCP)M-OCOOOR]$ are kinetically labile, readily exchanging their -OR functionalities with water, to afford equilibrium mixtures containing the corresponding alcohol R-OH and bicarbonates $[(iPrPCP)M-OCOOH]$. In the absence of CO₂, the bicarbonates are prone to undergo partial decarboxylation into the corresponding binuclear carbonates. These reactions are fully reversible, and the alkylcarbonate complexes are immediately regenerated if the required ROH and CO₂ are added to the system. In fact, equilibrium constant measurements demonstrate that the alkylcarbonate species $[(iPrPCP)M-OCOOOR]$ are very stable in solution, and thermodynamically favoured over the remaining species in equilibrium, namely, bicarbonates, carbonates, hydroxides or alkoxides. Provided that the enough ROH and CO₂ are present in the equilibrium, alkylcarbonates are always strongly prevalent, usually the only components detectable in the system. Therefore, if the M-OCOOOR linkage could be cleaved by alcohol to release hydroxide $[(iPrPCP)M-OH]$ and dialkylcarbonate, RO-CO-OR, carboxylation would occur catalytically, and reagents and products would attain their thermodynamic equilibrium concentrations. Unfortunately, our work has demonstrated conclusively that simple alcohols like MeOH are not competent to perform the nucleophilic displacement of the alkylcarbonate unit. Similar conclusions were reached also for a diol, ethyleneglycol, even though elimination of the cyclic ethylene carbonate would happen intramolecularly. Although Pd alkylcarbonates $[(iPrPCP)Pd-OCOOOR]$ decompose irreversibly when heated in the neat alcohols under high CO₂ pressures, their nickel counterparts survive even the under the harshest conditions, e. g.,

MeOH/sc-CO₂ showing that thermal instability is not the problem in this system. Conversely, methylcarbonate complexes [(ⁱPrPCP)M-OCOOMe] behave as mild nucleophiles towards electrophilic methylating reagents, Me-X, to yield dimethylcarbonate and the corresponding “inorganic” species, [(ⁱPrPCP)M-X]. Our study has shown that these reactions do involve true electrophilic attack, either at the metal centre or directly on the ligand, and not electron-transfer mechanisms. Thus, successful closure of the carboxylation catalytic cycle requires a catalyst that performs the simultaneous nucleophilic activation of CO₂, achieved at a basic alkoxo fragment, and electrophilic activation of the alcohol to become an alkyl transfer agent. The latter feature demands a strongly acidic active site, not available in our model system. These conclusions are in line with the fact that the best catalysts so far are metal alkoxides with a Lewis-acidic metal centre, and highlight the need for advanced catalyst design combining nearby basic and acid reactive sites in close proximity.

Experimental Section

All operations were carried out under oxygen free nitrogen atmosphere using conventional Schlenk techniques or a nitrogen-filled glove box. Solvents were rigorously dried and degassed before use. Microanalyses were performed by the Analytical Service of the Instituto de Investigaciones Químicas. NMR spectra were recorded on Bruker DPX-300, DRX-400 and DRX-500. Chemical shifts (δ) are in ppm. Solvents were used as internal standards for the reference of ¹H and ¹³C spectra, but chemical shifts are referenced with respect to TMS. ³¹P spectra are reported with respect to external H₃PO₄. Assignment of signals were assisted by combined one-dimensional (gated-¹³C) and two-dimensional 2D homonuclear ¹H-¹H COSY and phase-sensitive NOESY, and heteronuclear ¹³C-¹H HSQC and HMBC hetero-correlations. IR spectra were recorded on a Bruker Tensor 27 FTIR spectrophotometer. Abbreviations for multiplicities are as usual, and the letters b and v denote “broad” and “virtual”, respectively (e. g.: bm, broad multiplet, dvt = doublet of virtual triplets). Apparent constants for virtual couplings are marked with asterisk (*). Complexes [(ⁱPrPCP)M-X (M = Ni, X = Me, ¹⁹c I (15a), ¹⁹c OH (1a), ¹⁹a OMe (4a), ¹⁹b OEt (5), ¹⁹e OnBu (6), ¹⁹e OiPr (7), ¹⁹e OCH₂CH₂OH (8) ¹⁹e OTf (16a) ¹⁹c; M = Pd, X = Me, ¹⁹c I (15b), ¹⁹c OH (1b), ¹⁹a OMe (4b), ²⁰ OTf (16b) ¹⁹c) were prepared as previously described. Spectral simulations were carried out with gNMR.³³ GC-MS analyses were carried out in a ThermoQuest TRACE-GC Gas Chromatograph equipped with a TRB-1 capillary column and an Automass MULTI quadrupole mass detector in electron-impact mode.

Synthesis of Alkylcarbonates Complexes [(ⁱPrPCP)M-OCOOR] [M = Ni, R = Me (9a); Et, (10); nBu, (11); iPr, (12); CH₂CH₂OH, (13); M = Pd, R = Me (9b)].

These complexes were formed by reacting the corresponding alkoxides with CO₂. The alkylcarbonate products could not be

isolated in pure state due to their high solubility in common organic solvents and their facile decarboxylation during the evaporation process under vacuum, therefore they were characterized in solution by NMR spectroscopy.

The general procedure is illustrated with the preparation of compound 9a: This was prepared *in situ* by bubbling CO₂ into a solution of 4a in C₆D₆. The reaction is immediate, and it causes a colour change, from the characteristic orange of 4a to a yellow hue. The transformation is extremely clean, and the only by-product detected is the bicarbonate 2a, due to the presence of a small amount the hydroxide 1a.

Spectroscopic and analytical data for 9a/b, 10- 13:

9a: ¹H NMR (400.1 MHz, C₆D₆, 25 °C) δ 1.00 (dvt, 12H, ³J_{HH} \approx *J_{HP} \approx 6.9 Hz, CHMeMe); 1.40 (dvt, 12H, ³J_{HH} \approx *J_{HP} \approx 7.3 Hz, CHMeMe); 2.01 (m, 4H, CHMeMe); 2.66 (vt, 4H, *J_{HP} = 3.7 Hz, CH₂ (PCP)); 3.72 (s, 3H, OCH₃); 6.79 (d, 2H, ³J_{HH} = 7.3 Hz, C_{ar}H_m); 6.98 (t, 1H, ³J_{HH} = 7.3 Hz, C_{ar}H_p). ¹³C{¹H} NMR (100.6 MHz, C₆D₆, 25 °C): 18.0 (s, CHMeMe); 18.9 (s, CHMeMe); 23.7 (vt, *J_{CP} = 9.9 Hz, CHMeMe); 31.1 (vt, *J_{CP} = 13.2 Hz, CH₂ (PCP)); 53.0 (s, OCH₃); 122.4 (vt, *J_{CP} = 8.7 Hz, C_{ar}H_m); 125.4 (s, C_{ar}H_p); 152.2 (t, ²J_{CP} = 17.4 Hz, C_{ar-i}); 153.0 (vt, *J_{CP} = 13.1 Hz, C_{ar-o}); 158.1 (s, OCOO). ³¹P{¹H} NMR (162.0 MHz, C₆D₆, 25 °C): 56.5.

9b: ¹H NMR (400.1 MHz, C₆D₆, 25 °C) δ 0.92 (dvt, 12H, ³J_{HH} \approx *J_{HP} \approx 7.2 Hz, CHMeMe); 1.30 (dvt, 12H, ³J_{HH} \approx *J_{HP} \approx 7.8 Hz, CHMeMe); 2.07 (m, 4H, CHMeMe); 2.74 (vt, 4H, *J_{HP} = 3.7 Hz, CH₂ (PCP)); 3.81 (s, 3H, OCH₃); 6.90 (d, 2H, ³J_{HH} = 7.4 Hz, C_{ar}H_m); 7.00 (t, 1H, ³J_{HH} = 7.4 Hz, C_{ar}H_p). ¹³C{¹H} NMR (100.6 MHz, C₆D₆, 25 °C): 17.9 (s, CHMeMe); 18.8 (s, CHMeMe); 24.4 (vt, *J_{CP} = 10.7 Hz, CHMeMe); 32.0 (vt, *J_{CP} = 11.6 Hz, CH₂ (PCP)); 53.18 (s, OCH₃); 122.9 (vt, *J_{CP} = 10.4 Hz, C_{ar}H_m); 125.1 (s, C_{ar}H_p); 151.4 (vt, *J_{CP} = 10.7 Hz, C_{ar-o}); 154.5 (s, C_{ar-i}); 159.5 (s, OCOO). ³¹P{¹H} NMR (162.0 MHz, C₆D₆, 25 °C): 59.7.

10: ¹H NMR (300.1 MHz, C₆D₆, 25 °C) δ 1.02 (dvt, 12H, ³J_{HH} \approx *J_{HP} \approx 6.8 Hz, CHMeMe); 1.25 (t, 3H, ³J_{HH} = 7.0 Hz, CH₂Me); 1.42 (dvt, 12H, ³J_{HH} \approx *J_{HP} \approx 7.2 Hz, CHMeMe); 2.04 (m, 4H, CHMeMe); 2.67 (vt, 4H, *J_{HP} = 4.1 Hz, CH₂ (PCP)); 4.23 (c, 2H, ³J_{HH} = 7.0 Hz, OCH₂); 6.80 (d, 2H, ³J_{HH} = 7.4 Hz, C_{ar}H_m); 6.98 (t, 1H, ³J_{HH} = 7.4 Hz, C_{ar}H_p). ¹³C{¹H} NMR (75.5 MHz, C₆D₆, 25 °C): 15.8 (s, CH₂Me); 18.0 (s, CHMeMe); 18.8 (s, CHMeMe); 23.8 (vt, *J_{CP} = 9.8 Hz, CHMeMe); 31.1 (vt, *J_{CP} = 13.2 Hz, CH₂ (PCP)); 61.2 (s, OCH₂); 122.4 (vt, *J_{CP} = 8.6 Hz, C_{ar}H_m); 125.3 (s, C_{ar}H_p); 152.3 (t, ²J_{CP} = 17.5 Hz, C_{ar-i}); 153.0 (vt, *J_{CP} = 13.0 Hz, C_{ar-o}); 157.6 (s, OCOO). ³¹P{¹H} NMR (121.5 MHz, C₆D₆, 25 °C): 56.5.

11: ¹H NMR (500 MHz, C₆D₆, 25 °C) δ 1.02 (dvt, 12H, ³J_{HH} \approx *J_{HP} \approx 6.8 Hz, CHMeMe); 1.31 (d, 6H, ³J_{HH} = 6.0 Hz, CH(Me)₂); 1.41 (dvt, 12H, ³J_{HH} \approx *J_{HP} \approx 7.2 Hz, CHMeMe); 2.05 (m, 4H, CHMeMe); 2.67 (ma, CH₂ (PCP)); 5.05 (hept, 1H, OCH); 6.80 (d, 2H, ³J_{HH} = 7.5 Hz, C_{ar}H_m); 6.98 (t, 1H, ³J_{HH} = 7.4 Hz, C_{ar}H_p). ¹³C{¹H} NMR (125.7 MHz, C₆D₆, 25 °C): 18.0 (s, CHMeMe); 18.9 (s, CHMeMe); 23.1 (s, CH(Me)₂); 23.8 (vt, *J_{CP} = 9.9 Hz, CHMeMe); 31.1 (vt, *J_{CP} = 13.3 Hz, CH₂ (PCP)); 67.3 (s, OCH); 122.4 (vt, *J_{CP} = 8.6 Hz, C_{ar}H_m); 125.3 (s, C_{ar}H_p); 152.2 (t, ²J_{CP} = 17.0 Hz, C_{ar-i}); 153.1 (vt, *J_{CP} = 13.2 Hz, C_{ar-o}); 157.3 (s, OCOO). ³¹P{¹H} NMR (202.4 MHz, C₆D₆, 25 °C): 56.4.

12: ^1H NMR (300 MHz, C_6D_6 , 25 °C) δ 0.88 (t, 3H, $^3J_{\text{HH}} = 7.4$ Hz, CH_2Me); 1.02 (dvt, 12H, $^3J_{\text{HH}} \approx ^*J_{\text{HP}} \approx 7.0$ Hz, CHMeMe); 1.38 (m, 2H, CH_2Me); 1.38 (dvt, 12H, $^3J_{\text{HH}} \approx ^*J_{\text{HP}} \approx 7.1$ Hz, CHMeMe); 1.62 (m, 2H, $\text{CH}_2\text{CH}_2\text{Me}$); 2.03 (m, 4H, CHMeMe); 2.67 (vt, 4H, $^*J_{\text{HP}} = 4.2$ Hz, CH_2 (PCP)); 4.12 (c, 2H, $^3J_{\text{HH}} = 6.6$ Hz, OCH_2); 6.74 (d, 2H, $^3J_{\text{HH}} = 7.4$ Hz, $\text{C}_{\text{ar}}\text{H}_m$); 6.90 (t, 1H, $^3J_{\text{HH}} = 7.5$ Hz, $\text{C}_{\text{ar}}\text{H}_p$). $^{13}\text{C}\{^1\text{H}\}$ NMR (75.5 MHz, C_6D_6 , 25 °C): 14.1 (s, CH_2Me); 18.0 (s, CHMeMe); 18.8 (s, CHMeMe); 19.7 (s, CH_2Me); 23.8 (vt, $^*J_{\text{CP}} = 9.5$ Hz, CHMeMe); 31.1 (vt, $^*J_{\text{CP}} = 13.1$ Hz, CH_2 (PCP)); 32.4 (s, CH_2CH_2); 65.5 (s, OCH_2); 122.4 (vt, $^*J_{\text{CP}} = 8.1$ Hz, $\text{C}_{\text{ar}}\text{H}_m$); 125.3 (s, $\text{C}_{\text{ar}}\text{H}_p$); 152.3 (t, $^2J_{\text{CP}} = 17.3$ Hz, $\text{C}_{\text{ar-i}}$); 153.0 (vt, $^*J_{\text{CP}} = 13.0$ Hz, $\text{C}_{\text{ar-o}}$); 157.7 (s, OCOO). $^{31}\text{P}\{^1\text{H}\}$ NMR (121.5 MHz, C_6D_6 , 25 °C): 56.6.

13: ^1H NMR (300 MHz, C_6D_6 , 25 °C) 1.00 (dvt, 12H, $^3J_{\text{HH}} \approx ^*J_{\text{HP}} \approx 7.0$ Hz, CHMeMe); 1.40 (dvt, 12H, $^3J_{\text{HH}} \approx ^*J_{\text{HP}} \approx 7.1$ Hz, CHMeMe); 1.97 (m, 4H, CHMeMe); 2.64 (vt, 4H, $^*J_{\text{HP}} = 4.1$ Hz, CH_2 (PCP)); 3.59 (s, 1H, OH); 3.81 (m, 2H, CH_2OH); 4.17 (m, 2H, OCH_2); 6.77 (d, 2H, $^3J_{\text{HH}} = 7.3$ Hz, $\text{C}_{\text{ar}}\text{H}_m$); 6.97 (t, 1H, $^3J_{\text{HH}} = 7.4$ Hz, $\text{C}_{\text{ar}}\text{H}_p$). $^{13}\text{C}\{^1\text{H}\}$ NMR (75.5 MHz, C_6D_6 , 25 °C): 18.0 (s, CHMeMe); 18.8 (s, CHMeMe); 23.8 (vt, $^*J_{\text{CP}} = 9.7$ Hz, CHMeMe); 30.9 (vt, $^*J_{\text{CP}} = 12.8$ Hz, CH_2 (PCP)); 64.3 (s, CH_2OH); 68.4 (s, OCH_2); 122.5 (vt, $^*J_{\text{CP}} = 8.6$ Hz, $\text{C}_{\text{ar}}\text{H}_m$); 125.6 (s, $\text{C}_{\text{ar}}\text{H}_p$); 151.4 (s, $\text{C}_{\text{ar-i}}$); 153.1 (t, $^2J_{\text{CP}} = 12.7$ Hz, $\text{C}_{\text{ar-o}}$); 159.2 (s, OCOO). $^{31}\text{P}\{^1\text{H}\}$ NMR (121.5 MHz, C_6D_6 , 25 °C): 56.8.

Synthesis of Carbamate Complexes **14** [$^{\text{iPr}}\text{PCP}$]Ni-NPhCOOMe and **14'** [$^{\text{iPr}}\text{PCP}$]Ni-OCONHPh.

14: To a solution of 128 mg (0.3 mmol) of complex **4a** in 15 mL of hexane was added 36.1 μl (0.33 mmol) of phenyl isocyanate. The colour of the solution changed from orange to pale yellow. The solvent was then evaporated under reduced pressure, the residue was extracted with hexane, and the solution was filtered and concentrated. The product **14** crystallized (orange crystals) when the hexane solution was concentrated to 1 or 2 mL and cooled to -30 °C. Yield: 71%. ^1H NMR (300 MHz, C_6D_6 , 25 °C) 0.99 (m, 24H, CHMeMe); 1.84 (m, 4H, CHMeMe); 2.86 (vt, 4H, $^*J_{\text{HP}} = 3.5$ Hz, CH_2 (PCP)); 3.72 (s, 3H, OMe); 6.82 (d, 2H, $^3J_{\text{HH}} = 7.5$ Hz, $\text{C}_{\text{ar}}\text{H}_m$); 6.87 (t, 1H, $^3J_{\text{HH}} = 7.3$ Hz, $\text{C}_{\text{Ph}}\text{H}_p$); 6.96 (t, 1H, $^3J_{\text{HH}} = 7.5$ Hz, $\text{C}_{\text{ar}}\text{H}_p$); 7.28 (t, 2H, $^3J_{\text{HH}} = 7.9$ Hz, $\text{C}_{\text{Ph}}\text{H}_m$); 8.79 (d, 2H, $^3J_{\text{HH}} = 8.0$ Hz, $\text{C}_{\text{Ph}}\text{H}_o$). $^{13}\text{C}\{^1\text{H}\}$ NMR (75.5 MHz, C_6D_6 , 25 °C): 17.6 (s, CHMeMe); 19.1 (s, CHMeMe); 24.3 (vt, $^*J_{\text{CP}} = 9.0$ Hz, CHMeMe); 33.1 (vt, $^*J_{\text{CP}} = 12.8$ Hz, CH_2 (PCP)); 50.2 (s, OMe); 119.7 (s, $\text{C}_{\text{Ph}}\text{H}_p$); 121.8 (vt, $^*J_{\text{CP}} = 7.8$ Hz, $\text{C}_{\text{ar}}\text{H}_m$); 124.2 (s, $\text{C}_{\text{Ph}}\text{H}_o$); 125.6 (s, $\text{C}_{\text{ar}}\text{H}_p$); 127.8 (s, $\text{C}_{\text{Ph}}\text{H}_m$); 151.3 (vt, $^*J_{\text{CP}} = 11.6$ Hz, $\text{C}_{\text{ar-o}}$); 152.5 (s, $\text{C}_{\text{Ph-i}}$); 155.8 (t, $^2J_{\text{CP}} = 17.0$ Hz, $\text{C}_{\text{ar-i}}$); 158.4 (s, CO). $^{31}\text{P}\{^1\text{H}\}$ NMR (121.5 MHz, C_6D_6 , 25 °C): 52.6. IR (Nujol mull): $\nu(\text{C}=\text{O})$ 1648 cm^{-1} , $\nu(\text{C}-\text{O})$ 1082 cm^{-1} , $\nu(\text{C}-\text{N})$ 1331 cm^{-1} . Anal. Calcd for $\text{C}_{28}\text{H}_{42}\text{NiO}_3\text{P}_2$: C, 61.56; H, 7.93; N, 2.56. Found: C, 61.58; H, 7.99; N, 2.52.

14': This complex was characterized on the basis of its NMR spectra, without the isolation of the pure product. In an NMR tube, 10.3 mg (0.025 mmol) of hydroxide **1a** was dissolved in C_6D_6 and their ^1H and $^{31}\text{P}\{^1\text{H}\}$ NMR spectra were registered. After the addition of 2.2 μl (0.027 mmol) of phenyl isocyanate into the NMR tube, the quantitative formation of a new product was observed, for which we propose the structure [$^{\text{iPr}}\text{PCP}$]Ni-OCONHPh (**14'**). ^1H NMR (500 MHz, C_6D_6 , 25 °C) 1.01 (dvt, 12H,

$^3J_{\text{HH}} \approx ^*J_{\text{HP}} \approx 6.9$ Hz, CHMeMe); 1.41 (dvt, 12H, $^3J_{\text{HH}} \approx ^*J_{\text{HP}} \approx 7.3$ Hz, CHMeMe); 1.99 (m, 4H, CHMeMe); 2.69 (vt, 4H, $^*J_{\text{HP}} = 3.8$ Hz, CH_2 (PCP)); 6.82 (d, 2H, $^3J_{\text{HH}} = 7.4$ Hz, $\text{C}_{\text{ar}}\text{H}_m$); 6.85 (t, 1H, $^3J_{\text{HH}} = 7.6$ Hz, $\text{C}_{\text{Ph}}\text{H}_p$); 7.00 (t, 1H, $^3J_{\text{HH}} = 7.4$ Hz, $\text{C}_{\text{ar}}\text{H}_p$); 7.24 (t, 2H, $^3J_{\text{HH}} = 7.9$ Hz, $\text{C}_{\text{Ph}}\text{H}_m$); 7.75 (d, 2H, $^3J_{\text{HH}} = 8.5$ Hz, $\text{C}_{\text{Ph}}\text{H}_o$). $^{13}\text{C}\{^1\text{H}\}$ NMR (125.7 MHz, C_6D_6 , 25 °C): 17.7 (s, CHMeMe); 18.5 (s, CHMeMe); 23.6 (vt, $^*J_{\text{CP}} = 9.8$ Hz, CHMeMe); 30.9 (vt, $^*J_{\text{CP}} = 13.1$ Hz, CH_2 (PCP)); 117.0 (s, $\text{C}_{\text{Ph}}\text{H}_p$); 119.0 (s, $\text{C}_{\text{Ph}}\text{H}_o$); 122.1 (vt, $^*J_{\text{CP}} = 8.5$ Hz, $\text{C}_{\text{ar}}\text{H}_m$); 124.9 (s, $\text{C}_{\text{ar}}\text{H}_p$); 128.5 (s, $\text{C}_{\text{Ph-m}}$); 143.2 (s, $\text{C}_{\text{Ph-i}}$); 152.5 (vt, $^*J_{\text{CP}} = 13.0$ Hz, $\text{C}_{\text{ar-o}}$); 152.6 (t, $^2J_{\text{CP}} = 17.7$ Hz, $\text{C}_{\text{ar-i}}$); 158.3 (s, CO).

Independent syntheses of Tosylate Complexes **17a/b**.

These compounds were prepared from the methyl complexes [$^{\text{iPr}}\text{PCP}$]M(Me) following a similar procedure to that described before for the analogous triflate derivatives **16a/b**.^{19c} Below is described the synthesis for compound **17a**: To a solution of 114 mg (0.21 mmol) of [$^{\text{iPr}}\text{PCP}$]Ni(Me) in 15 mL of THF cooled at -30 °C was added 40 mg of *p*-toluenesulfonic acid (HOTs) in 5 mL THF. The mixture was allowed to warm to the room temperature, and was taken dryness under vacuum. The solid residue was recrystallized from Et_2O at -20 °C. Yield: 64%. ^1H NMR (400.1 MHz, C_6D_6 , 25 °C) 0.91 (dvt, 12H, $^3J_{\text{HH}} \approx ^*J_{\text{HP}} \approx 6.9$ Hz, CHMeMe); 1.53 (dvt, 12H, $^3J_{\text{HH}} \approx ^*J_{\text{HP}} \approx 7.9$ Hz, CHMeMe); 1.96 (s, 3H, CH_3); 2.27 (m, 4H, CHMeMe); 2.62 (vt, 4H, $^*J_{\text{HP}} = 3.6$ Hz, CH_2 (PCP)); 6.74 (d, 2H, $^3J_{\text{HH}} = 7.4$ Hz, $\text{C}_{\text{Tot}}\text{H}_m$); 6.89 (d, 2H, $^3J_{\text{HH}} = 7.8$ Hz, $\text{C}_{\text{ar}}\text{H}_m$); 6.95 (t, 1H, $^3J_{\text{HH}} = 7.4$ Hz, $\text{C}_{\text{Ph}}\text{H}_p$); 8.03 (d, 2H, $^3J_{\text{HH}} = 8.1$ Hz, $\text{C}_{\text{Tot}}\text{H}_o$). $^{13}\text{C}\{^1\text{H}\}$ NMR (100.6 MHz, C_6D_6 , 25 °C): 18.3 (s, CHMeMe); 19.5 (s, CHMeMe); 21.1 (s, CH_3); 24.0 (vt, $^*J_{\text{CP}} = 10.1$ Hz, CHMeMe); 30.0 (vt, $^*J_{\text{CP}} = 13.5$ Hz, CH_2 (PCP)); 122.7 (vt, $^*J_{\text{CP}} = 8.5$ Hz, $\text{C}_{\text{ar}}\text{H}_m$); 125.8 (s, $\text{C}_{\text{ar}}\text{H}_p$); 126.6 (s, $\text{C}_{\text{Tot}}\text{H}_m$); 128.7 (s, $\text{C}_{\text{Tot}}\text{H}_o$); 139.6 (s, $\text{C}_{\text{Tot-i,p}}$); 143.5 (s, $\text{C}_{\text{Tot-i,i}}$); 147.7 (t, $^2J_{\text{CP}} = 17.0$ Hz, $\text{C}_{\text{ar-i}}$); 153.1 (vt, $^*J_{\text{CP}} = 12.3$ Hz, $\text{C}_{\text{ar-o}}$). $^{31}\text{P}\{^1\text{H}\}$ NMR (202.4 MHz, C_6D_6 , 25 °C): 58.8. IR (Nujol mull): $\nu(\text{S}-\text{O})$ 1159 cm^{-1} , 1113 cm^{-1} , 1002 cm^{-1} . Anal. Calcd for $\text{C}_{27}\text{H}_{42}\text{NiO}_3\text{P}_2\text{S}$: C, 57.16; H, 7.46; S, 5.65. Found: C, 57.39; H, 7.17; S, 5.56.

17b: This was obtained similarly to its Ni analogue in 70% yield. ^1H NMR (500 MHz, C_6D_6 , 25 °C) 0.87 (dvt, 12H, $^3J_{\text{HH}} \approx ^*J_{\text{HP}} \approx 7.0$ Hz, CHMeMe); 1.41 (dvt, 12H, $^3J_{\text{HH}} \approx ^*J_{\text{HP}} \approx 7.9$ Hz, CHMeMe); 1.98 (s, 3H, CH_3); 2.29 (m, 4H, CHMeMe); 2.70 (bs, 4H, CH_2 (PCP)); 6.88 (d, 2H, $^3J_{\text{HH}} = 7.3$ Hz, $\text{C}_{\text{Tot}}\text{H}_m$); 6.92 (d, 2H, $^3J_{\text{HH}} = 7.7$ Hz, $\text{C}_{\text{ar}}\text{H}_m$); 6.99 (t, 1H, $^3J_{\text{HH}} = 7.3$ Hz, $\text{C}_{\text{Ph}}\text{H}_p$); 8.17 (d, 2H, $^3J_{\text{HH}} = 7.8$ Hz, $\text{C}_{\text{Tot}}\text{H}_o$). $^{13}\text{C}\{^1\text{H}\}$ NMR (125.7 MHz, C_6D_6 , 25 °C): 17.7 (s, CHMeMe); 18.9 (s, CHMeMe); 20.7 (s, CH_3); 24.2 (vt, $^*J_{\text{CP}} = 10.9$ Hz, CHMeMe); 30.9 (vt, $^*J_{\text{CP}} = 11.7$ Hz, CH_2 (PCP)); 123.0 (vt, $^*J_{\text{CP}} = 10.5$ Hz, $\text{C}_{\text{ar}}\text{H}_m$); 125.2 (s, $\text{C}_{\text{ar}}\text{H}_p$); 126.6 (s, $\text{C}_{\text{Tot}}\text{H}_m$); 128.4 (s, $\text{C}_{\text{Tot}}\text{H}_o$); 139.1 (s, $\text{C}_{\text{Tot-i,p}}$); 143.7 (s, $\text{C}_{\text{Tot-i,i}}$); 151.0 (vt, $^*J_{\text{CP}} = 10.1$ Hz, $\text{C}_{\text{ar-o}}$); 151.6 (s, $\text{C}_{\text{ar-i}}$). $^{31}\text{P}\{^1\text{H}\}$ NMR (162.0 MHz, C_6D_6 , 25 °C): 61.7. IR (Nujol mull): $\nu(\text{S}-\text{O})$ 1152 cm^{-1} , 1112 cm^{-1} , 1001 cm^{-1} . Anal. Calcd for $\text{C}_{27}\text{H}_{42}\text{O}_3\text{P}_2\text{S}$: C, 52.73; H, 6.88; S, 5.21. Found: C, 52.91; H, 6.99; S, 4.99.

Transformation of Alkylcarbonate **4a** into Carbonate **3a**.

0.025 mmol of complexes **4a** or **6** were dissolved in 0.6 mL of toluene- d_8 and transferred to an NMR tube capped with a rubber septum. The septum was pierced with a thin hypodermic needle to enable slow gas exchange. A Schlenk tube, capped with a unpierced Sub-a-Seal™ septum, was flushed with N_2 and

placed in a thermostatic oil bath at 100 °C. Once its temperature was stabilized, the Schlenk tube was opened and the NMR sample was introduced inside in N₂ counterflow. The system was closed and the Suba-a-Seal septum was pierced with a needle. The N₂ flow was then adjusted to 2 cc/min with an accurate flow regulator. The system was carefully opened at regular intervals, and the sample was removed from the tube to record its NMR spectra (¹H and ³¹P{¹H}) as described in the text.

To confirm that free alcohol is the only organic product of the alkylcarbonate decarboxylation, a solution of compound **9a** in C₆D₆, generated from 12 mg (0.025 mmol) of complex **4a**, was evaporated under reduced pressure. The volatile components were collected in a small trap cooled with liquid nitrogen. The solid residue was analyzed by ³¹P{¹H} NMR, that showed a 1:5 mixture of **9a** and **3a**, while the ¹H NMR spectrum and GC analysis of the condensate recovered from the trap revealed only methanol in C₆D₆.

Reactions of Carbonates (**3a/b**) with methanol.

The reactions of carbonate complexes (**3a/b**) with MeOH were investigated by NMR spectroscopy using NMR tubes fitted with gas-tight Teflon valves. The samples (solutions of the corresponding carbonate complexes in C₆D₆ with a specific amount of MeOH) were prepared in a glove-box.

Titration of Alkylcarbonate (**9a/b**) Complexes with Alcohols.

The reversible reactions of bicarbonate complexes (**2a/b**) with alcohols were performed in regular, septum-capped NMR tubes, using C₆D₆ as solvent. Alcohols used in this protocol were dried by distillation from the corresponding sodium alkoxides, generated *in situ* by dissolving pieces of sodium in the alcohol prior to the distillation. The following experimental protocol was applied: In the glovebox, an amount close to 0.025 mmol (**2a**: 11.4 mg; **2b** 11.9 mg) of the corresponding bicarbonate was accurately weighed in an analytical balance. The sample was dissolved in 0.6 mL of C₆D₆ and transferred to an NMR tube capped with a rubber septum. A second septum-capped NMR tube was used to store the required alcohol. The tubes were taken from the box, and ³¹P{¹H} and ¹H NMR spectra of the complex sample solution were recorded on the 300 MHz NMR spectrometer. With gastight syringes of suitable volume, increasing amounts of the alcohol were taken from the reservoir tube and successively added to the sample of the complex (e.g., 0.5, 1.5, 3.5, 6.5 μL, etc). After each addition, the sample was gently shaken, returned to the NMR probe, and the ³¹P{¹H} spectra were recorded. Control experiments were performed to check that the equilibration of the species was essentially instantaneous. The equilibrium constant *K*₁ was calculated as [MOCOOR]/[MOCOOH] × [H₂O]/[ROH] for each addition. The alkylcarbonate to bicarbonate ratio was directly obtained from the ³¹P integrals, and the ratio of water to alcohol was deduced from the total amount of alcohol added using stoichiometry relationships.

To investigate the reaction between complex **9a** and EtOH the same protocol was applied, but in this case the alkylcarbonate

sample was prepared *in situ* bubbling CO₂ into a solution of complex **4a**.

Attempted carboxylation of alcohols using **1a** or **1b** as catalysts.

The following experiments were designed to determine the potential formation of organic carbonates.

a) pressure NMR tube experiments: In the glove box, samples of the Ni or Pd hydroxides **1a** or **1b**, respectively (*ca.* 0.025 mmol), were dissolved in dry methanol (0.6 mL) and transferred to thick-walled glass NMR tubes provided with screw PTFE valves and Swagelock-type fittings for 1/16" steel tube. These were taken from the glove box, attached to a pressure line and flushed three times with CO₂. In the last cycle, the pressure was set to 4 bar. The ³¹P{¹H} NMR spectra confirmed that the conversion of hydroxides **1a** and **1b** into the methylcarbonates **9a** and **9b**, respectively, was complete. In two series of experiments, the samples were heated at 80 °C or 100 °C for 24 h, after which time the samples were analyzed by ³¹P{¹H} NMR and GC-MS. A similar experiment was conducted with **1a** using 4 bar of a 3:1 CO₂/¹³CO₂ (25 % ¹³C) in methanol-*d*₄, and and 0.01 ml of dimethyl carbonate were added. ¹³C{¹H} spectra taken above and after the experiment showed no enhancement of the carbonyl signal of dimethyl carbonate.

b) Medium pressure experiments: A 50 mL steel reactor was charged with **1a** or **1b** (0.1 mmol) in 15 ml of methanol. The reactor was purged with CO₂ and pressurized with the same gas at 20 bar. Then it was heated at 100 °C for 24 h, after which time it was cooled down, and the pressure was carefully vented.

c) sc-CO₂ experiments: The reactor, once degassed and purged with CO₂ was loaded with a solution containing 0.2 mmol of the complex (**1a** or **1b**) and 0.25 ml (2.35 mmol) of toluene as internal standard. Next, 15 mL of liquid CO₂ were pumped in, and the reactor was heated to 100 °C for 2 h. The pressure rose up to 170 bar. The system was then cooled to -80 °C and carefully vented.

The solutions obtained in all experiments were analyzed using GC-MS techniques. These analyses ruled out net production organic carbonates. In all experiments with Pd, a dark suspension was invariably formed and the ³¹P{¹H} spectra showed that the pincer framework does not survive the conditions used.

Reactions of Alkylcarbonate (**9a/b**) Complexes with Alkylating Agents (MeI, MeOTf, MeOTs).

These reactions were studied by ³¹P{¹H} NMR spectroscopy. The identity of the products was established by comparison with ³¹P data for authentic samples. NMR samples of the alkylcarbonates (**9a/b**) were prepared dissolving 0.025 mmol of the corresponding methoxide (**4a/b**) in C₆D₆ inside the globe-box. Then, the samples were transferred to NMR tubes, and CO₂ was bubbled into the solution. The prescribed amount of alkylating agent (1, 10, 15 or 20 eqs) was added to each solution with the help of a micro syringe, then solvent was added to adjust a fixed volume (0.6 ml) and the tubes were sealed. In the cases the reactions were fast enough, the reactions were carried out in the

NMR probe, pre-heated at 60 °C and monitored continuously. For slower reactions, the samples were placed in a therstatic in an oil bath, and the spectra were recorded each 6-12 h.

Reactions of 9a,b with 6-iodo-1-hexene.

These reactions were investigated as described above except that the alkylating reagent was 6-iodo-1-hexene, and the **9**: alkyl iodide was 1:2. The samples were heated in an oil bath at 100 °C, and they were taken at regular intervals to perform NMR analyses until all the starting material was consumed. 6-iodo-1-hexene was prepared from 5-hexen-1-ol following a literature synthetic method.³⁴

Computational Details.

All calculations were performed with the Spartan'16 software package.³⁵ The approach used was the same described before.^{19e} The structures of all complexes involved in the CO₂ exchange reaction shown in Scheme 7 were modelled without simplifications, using the experimental X-ray diffraction data as the initial guess for bicarbonates **2a** and **2b**, and adding the corresponding R groups for alkylcarbonates. Models for the hydroxide and alkoxide complexes were taken as previously reported.^{18e} Geometry optimizations and vibrational analyses were carried out with the PBE functional and the 6-31G* basis set for nickel complexes, and LACVP* for the Pd series. The latter comprises the same 6-31G* functions for light elements and the LANL2DZ pseudopotential for Pd. Solvent effects (benzene) were included in the optimization procedure with the CPCM implicit model, setting the Bondi-type PCM radii for Ni and Pd as 2.28 and 2.48 Å, respectively. Electronic (SCF) energies were refined with a single point calculation at the PBE/6-311++G(3df,2p)/CPCM level. At this level of the theory, Spartan uses the all-electron def2-TZVP basis set to describe the Pd atom. Single-point calculations were accelerated using the "dual" option, that specifies that SCF convergence is achieved at the 6-311G* level, and then corrected perturbatively for the effect of additional diffuse and polarization functions. The final ΔG° and ΔE values for each molecular model were obtained adding the thermal and ZPE corrections from the 6-31G* calculation, respectively (thermal correction = $\Delta G^\circ - E(\text{SCF})$).

Conflicts of interest

There are no conflicts to declare.

Acknowledgements

The Spanish Ministerio de Economía y Competitividad (MINECO) and the FEDER funds of the European Union (CTQ2015-68978-P) supported this work. We warmly thank Prof. David J. Cole-Hamilton (St. Andrews University, UK) for the use of reactor facilities to investigate the reactions of hydroxides **1a** and **1b** with methanol in sc-CO₂.

Notes and references

- (a) M. Aresta, A. Dibenedetto, *Dalton Trans.* 2007, 2975. (b) D. J. Darensbourg, *Inorg. Chem.* 2010, **49**, 10765. (c) S. Huang, B. Yan, S. Wang, X. Ma, *Chem. Soc. Rev.* 2015, **44**, 3079.
- (a) M. Cokoja, M. E. Wilhelm, M. H. Anthofer, W. A. Herrmann, F. E. Kühn, *ChemSusChem* 2015, **8**, 2436. (b) M. R. Kember, A. Buchard, C. K. Williams, *Chem. Commun.* 2011, **47**, 141.
- G. Sienel, R. Rieth, K. T. Rowbottom, *In Ullmann's Encyclopedia of Industrial Chemistry*; Wiley-VCH: 2000.
- M. Aresta, A. Dibenedetto, A. Angelini, I. Pápai, *Top. Catal.* 2015, **58**, 2.
- Handbook of Green Chemistry and Technology*; J. Clark, D. Mcquarrie, Eds.; Blackwell Publishing: Oxford, 2002.
- (a) M. Aresta, A. Dibenedetto, C. Pastore, *Inorg. Chem.* 2003, **42**, 3256. (b) Q. Cai, B. Lu, L. Guo, Y. Shan, *Catal. Commun.* 2009, **10**, 605.
- (a) A. Dibenedetto, M. Aresta, A. Angelini, J. Ethiraj, B. M. Aresta, *Chem. Eur. J.* 2012, **18**, 10324. (b) M. Aresta, A. Dibenedetto, C. Pastore, A. Angelini, B. Aresta, I. Pápai, *J. Catal.* 2010, **269**, 44. (c) M. Aresta, A. Dibenedetto, C. Pastore, C. Cuocci, B. M. Aresta, E. De Giglio, *Catal. Today* 2008, **137**, 125. (d) Y. Yoshida, Y. Arai, S. Kado, K. Kunimori, K. Tomishige, *Catal. Today* 2006, **115**, 95. (e) K. Tomishige, Y. Ikeda, T. Sakai, K. Fujimoto, *J. Catal.* 2000, **192**, 355.
- (a) Q. Cai, H. Jin, B. Lu, H. Tangbo, Y. Shan, *Catal. Lett.* 2005, **103**, 225. (b) S. Fujita, B. M. Bhanage, Y. Ikushima, M. Arai, *Green Chem.* 2001, **3**, 87.
- (a) F. D. Bobbink, W. Guruszka, M. Hulla, S. Das, P. J. Dyson, *Chem. Commun.* 2016, **52**, 10787. (b) M. Aresta, A. Dibenedetto, E. Fracchiolla, P. Giannocaro, C. Pastore, I. Pápai, G. Schubert, *J. Org. Chem.* 2005, **70**, 6177.
- (a) K. Kohno, J.-C. Choi, Y. Oshima, H. Yasuda, T. Sakakura, *ChemSusChem* 2008, **1**, 186. (b) M. Ruf, F. A. Schell, R. Walz, H. Vahrenkamp, *Chem. Ber. / Recueil* 1997, **130**, 101.
- (a) M. Poor Kalhor, H. Chermette, S. Chambrey, D. Ballivet-Tkatchenko, *Phys. Chem. Chem. Phys.* 2011, **13**, 2401. (b) G. Laurency, M. Picquet, L. Plasseraud, *J. Organomet. Chem.* 2011, **696**, 1904. (c) T. Sakakura, J.-C. Choi, Y. Saito, T. Sako, *Polyhedron* 2000, **19**, 573. (d) D. Ballivet-Tkatchenko, O. Dousteau, S. Stutzmann, *Organometallics* 2000, **19**, 4563. (e) G. Laurency, A. F. Dalebrook, M. Picquet, L. Plasseraud, *J. Organomet. Chem.* 2015, **796**, 53.
- (a) M. Aresta, A. Dibenedetto, C. Pastore, I. Pápai, G. Schubert, *Top. Catal.* 2006, **40**, 71. (b) A. Dibenedetto, C. Pastore, M. Aresta, *Catal. Today* 2006, **115**, 88.
- M. Pool Kahlor, H. Chermette, D. Ballivet-Tkatchenko, *Polyhedron* 2012, **32**, 73.
- M. Aresta, A. Dibenedetto, L. Gianfrate, C. Pastore, *J. Mol. Catal. A: Chem.* 2003, **204**, 245.
- R. D. Simpson, R. G. Bergman, *Organometallics* 1992, **11**, 4306.
- D. J. Darensbourg, W. -Z. Lee, A. L. Phelps, E. Guidry, *Organometallics* 2003, **22**, 5585.
- (a) *Pincer Compounds, Synthesis and Applications*. D. Morales-Morales. Elsevier, Amsterdam, 2018. (b) S. Murugesan, K. Kirchner, *Dalton Trans.* 2018, **45**, 416. (c) *Pincer and Pincer-Type Complexes: Applications in Organic Synthesis and Catalysis*; K. J. Szabo, O. F. Wendt, Eds.; VCH, 2014. (d) *Organometallic Pincer Complexes*; G. van Koten, D. Milstein, Eds.; Springer: Berlin Heidelberg, 2013. (e) *The Privileged Pincer-Metal Platform: Coordination Chemistry & Applications*; G. van Koten, R. A. Gossage, Eds.; Springer: Berlin Heidelberg, 2016.
- For some relevant examples, see: (a) D. Huang, O. Makhlynets, L. L. Tan, S. C. Lee, E. V. Rybak-Akimova, R. H. Holm, *Proc. Nat. Acad. Sci.* 2010, **108**, 1222. (b) D. Huang, O. Makhlynets, L. L. Tan, S. C. Lee, E. V. Rybak-Akimova, R. H. Holm, *Inorg. Chem.* 2011, **50**, 10070. (c) H. W. Suh, T. J. Smeier, N. Hazari, R. A. Kemp, M. K. Tankase, *Organometallics*, 2012, **31**,

8225. (d) Y. E. Kim, S. Oh, S. Kim, O. Kim, J. Kim, S. W. Han, Y. Lee. *J. Am. Chem. Soc.* 2015, **137**, 4280. (e) S. Oh., S. Kim, D. Lee, J. Gwak, Y. Lee, *Inorg. Chem.* 2016, **55**, 12863. (f) H. Mousa, J. Bendix, O. F. Wendt, *Organometallics*, 2018, **37**, 2581. (g) K. J. Jonasson, A. H. Mousa, O. F. Wendt, *Polyhedron*, 2018, **143**, 132.
- 19 (a) J. Cámpora, P. Palma, D. Del Río, E. Álvarez, *Organometallics* 2004, **23**, 1652. (b) J. Cámpora, P. Palma, D. Del Río, M. M. Conejo, E. Álvarez, E. *Organometallics* 2004, **23**, 5653. (c) L. M. Martínez-Prieto, C. Melero, D. Del Río, P. Palma, J. Cámpora, E. Álvarez, *Organometallics* 2012, **31**, 1425. (d) Martínez-Prieto, L. M.; Real, C.; E. Ávila, E. Álvarez, P. Palma, J. Cámpora, *Eur J. Inorg. Chem.* 2013, 5555. (e) L. M. Martínez-Prieto, P. Palma, E. Álvarez, J. Cámpora, *Inorg. Chem.* 2017, **56**, 13086.
- 20 (a) C. Melero, L. M. Martínez-Prieto, P. Palma, D. Del Río, E. Álvarez, J. Cámpora, *J. Chem. Commun.* 2010, **40**, 8851. (b) L. M. Martínez-Prieto, E. Ávila, P. Palma, E. Álvarez, J. Cámpora, *Chem. Eur. J.* 2015, **21**, 9833.
- 21 a) J. Cámpora, I. Matas, P. Palma, E. Álvarez, C. Graiff, A. Tiri-picchio *Organometallics* 2007, **26**, 3840. b) J., Ruiz, M. T. Martínez, F. Florenciano, V. Rodríguez, G. López, P. A. Chalonnier, P. B. Hitchcock, *Inorg. Chem.* 2003, **42**, 3650. c) Hevia, E.; Pérez, J.; Riera, L.; Riera, V.; del Río, I.; García-Granda, S.; Miguel, D. *Chem. Eur. J.*, 2002, **8**, 4510. c) D. S. Glueck, L. J. Newman-Winslow, R. G. Bergman *Organometallics*, 1991, **10**, 1462.
- 22 Depending, of course, on the existence of stable carbonate complexes. See for example ref. 10b.
- 23 Although not explicitly reported, on the basis of published data it is very likely that the hydrolysis of a bismuth(III) methylcarbonate stabilized by a dianionic pincer ligand would afford the corresponding binuclear carbonate. See: S. F. Yin, J. Maruyama, T. Yamashita, S. Shimada, *Angew. Chem. Int. Ed.* 2008, **47**, 6590.
- 24 A. Dibenedetto, M. Aresta, P. Giannocaro, C. Pastore, I. Pápai, G. Schubert *Eur. J. Inorg. Chem.* 2006, 908.
- 25 M. B. Smith, J. March, Chapter 9 in *March's Advanced Organic Chemistry. Reactions, Mechanism, and Structure*, John Wiley & Sons: Hoboken, New Jersey, USA, 2007.
- 26 X. Hu, *Chem. Sci.* 2011, **2**, 1867.
- 27 See ref. 24, pp 504-505
- 28 D. Griller, K. U. Ingold, *Acc. Chem. Res.* 1980, **13**, 317.
- 29 B. M. Trost, M. R. Machacek, Z. T. Ball, *Org. Lett.* 2003, **5**, 1895.
- 30 T. Laube, A. Weidenhaupt, R. Hunziker, *J. Am. Chem. Soc.* 1991, **113**, 2561.
- 31 H. Zhang, A. Lei, *Dalton Trans.* 2011, **40**, 8745.
- 32 N. M. Camasso, M. S. Sanford, *Science* 2015, **347**, 1218.
- 33 Budzelaar, P. H. M. gNMR, NMR simulation software, available in the web at <https://home.cc.umanitoba.ca/~budzelaa/gNMR/gNMR.html>.
- 34 D. M. Hodgson, A. H. Labande, F. Y. T. M. Pierard, M. A. E. Castro, *J. Org. Chem.* 2003, **68**, 6153.
- 35 *Spartan'16*, Wavefunction, Inc. Irvine, CA, USA. Version 2.0.8., 2017.